New ozone-nitrogen model shows early senescence onset is the primary cause of ozone-induced reduction in grain quality of wheat

Jo Cook[1], Clare Brewster[2], Felicity Hayes[2], Nathan Booth[1], Sam Bland[3], Pritha Pande[3], Samarthia Thankappan[1], Håkan Pleijel[4], Lisa Emberson[1]

5   [1]Environment & Geography Dept., University of York, YO10 5DD, UK
[2]UK Centre for Ecology & Hydrology, Environment Centre Wales, Bangor, Wales, UK
[3]Stockholm Environment Institute at York, Environment & Geography Dept., University of York, YO10 5DD, UK
[4]Biological and Environmental Sciences Dept., University of Gothenburg, SE-40530, Sweden

Correspondence to: Jo Cook (jo.cook@york.ac.uk)

10   **Abstract.** Ozone (O_3) air pollution is well known to adversely affect both the grain and protein yield of wheat, an important staple crop. This study aims to identify and model the key plant processes influencing the effect of O_3 on wheat protein. We modified the DO_3SE-Crop model to incorporate nitrogen (N) processes, and parameterised the O_3 effect on stem, leaf and grain N using O_3 fumigation datasets spanning 3 years and 4 O_3 treatments. The modifications make the newly developed DO_3SE-CropN model the first crop model to include O_3 effects on N processes, making it a valuable tool for understanding O_3 effects on wheat quality. Our results show the new model captures the O_3 effect on grain N concentrations, and anthesis leaf and stem concentration well, with an R^2 of 0.6 for the increase in grain N concentration and an R^2 of 0.3 for the decrease in grain N content under O_3 exposure. However, the O_3 effect on harvest leaf and stem N is exaggerated. Overestimations of harvest leaf N range from ~20-120%, while overestimations of harvest stem N range from ~40-120%. Further, a sensitivity analysis revealed that, irrespective of O_3 treatment, early senescence onset (simulated as being ~13 days earlier in the very high vs low 20 O_3 treatment) was the primary plant process affecting grain N. This finding has implications for the breeding of stay-green cultivars for maintaining yield, as well as quality, under O_3 exposure. This modelling study therefore demonstrates the capability of the DO_3SE-CropN model to simulate processes by which O_3 affects N content, and thereby determines that senescence onset is the main driver of O_3 reductions in grain protein yield. The implication of the sensitivity analysis is that breeders should focus their efforts on stay-green cultivars that do not experience a protein penalty when developing O_3 tolerant 25   lines, to maintain both wheat yield and nutritional quality under O_3 exposure. This work supports the second phase of the tropospheric O_3 assessment report (TOAR) by investigating the impacts of tropospheric O_3 on wheat, with a focus on wheat quality impacts that will subsequently affect human nutrition.

1. Introduction

The first phase of the tropospheric ozone (O_3) assessment report (TOAR) (https://igacproject.org/activities/TOAR/TOAR-I) 30   built the world's largest database of surface O_3 metrics to identify global distribution of the pollutant and trends in O_3

concentrations over time. The second phase of TOAR (https://igacproject.org/activities/TOAR/TOAR-II), to which this paper contributes, has a broader scope, with one of the additional aims being to investigate the impact of tropospheric O_3 on human health and vegetation. The present work will address these goals by developing impact assessment methods that consider the interaction between O_3 and nitrogen (N) in crops. As N is a key component of protein, effects of O_3 on N have the potential to impact crop quality, and, as a result, human nutrition. Areas for further investigation to provide deeper understanding of O_3-N interactions are identified, and recommendations for future work to mitigate the negative effects of O_3 on both crop yield and protein are discussed.

1.1 The importance of wheat for nutrition and the threat of O_3

The Food and Agricultural Organisation of the United Nations (FAO) projects that staple cereals will play a critical role in ensuring food security; particularly in Central and West Asia, and North Africa where wheat provides at least 40% and 47% of dietary calories and protein respectively, compared to ~20% of dietary calories and protein globally (FAO, 2017). There is a large body of evidence, including work from the first phase of TOAR, suggesting that current ambient ozone (O_3) concentrations in key wheat growing locations are causing substantial productivity losses of equal importance to other, more well known, biotic and abiotic stresses (Mills et al., 2018a; Emberson et al., 2009; Mills et al., 2018c). Globally, wheat production is reduced by ~7%, though in some regions with high ambient O_3 concentrations, such as Northern India, the yield loss is much greater (> 15%) (Mills et al., 2018a). There is also a growing body of literature showing that O_3 affects the nutritional quality of the wheat grain and reduces the protein yield (Broberg et al., 2015; Piikki et al., 2008; Yadav et al., 2020, 2019a). Over the next century, increases to global population and economic growth, and changes to climate and land use, will increase emissions of O_3 precursors (NO_x and VOCs) (Fowler et al., 2008). For shared socio-economic pathway (SSP) 3-70 (often termed the "business-as-usual" scenario), projections show that O_3 concentrations will increase in most locations globally, particularly South and East Asia, South America, Africa and the middle East (Szopa et al., 2021). Alterations to local meteorology and carbon dioxide (CO_2) concentrations under climate change will also influence O_3 production (Fu and Tian, 2019), with Zanis et al. (2022) finding that for regions close to emissions sources climatic conditions will likely increase O_3 production. Understanding O_3 impact on the supply and nutritional quality of wheat grown in regions where O_3 concentrations are high/ predicted to increase is crucial (FAO et al., 2020). This will help us understand and address the threats posed by O_3 pollution on the ability of future wheat production to meet increasing demand and nutrient requirements (Shiferaw et al., 2013; Mills et al., 2018b).

1.2 The impact of O_3 on wheat quality and the mechanisms by which damage occurs

Reactive oxygen species (ROS), formed from O_3 entering the leaves through the stomata, trigger a series of reactions that reduce grain yield and quality (Emberson et al., 2018; Broberg et al., 2015). The uptake and remobilisation of nutrients under O_3 exposure is affected less severely by O_3 than the O_3-induced reduction in dry matter (DM). This results in a decrease in the nutrient yield of the grains (gNutrient m^{-2}) but an increase in the nutrient concentration (gNutrient gDM^{-1}) (Wang and Frei,

2

2011; Broberg et al., 2015). Broberg et al. (2015) further found that an increased grain protein concentration caused the baking properties, quantified by the Zeleny value, Hagberg falling number and dry and wet gluten content, to be positively affected by O_3. In some wheat studies, where O_3 concentrations are very high, grain protein concentration is decreased, potentially as a result of N being used for antioxidant production and defence against O_3 (Baqasi et al., 2018; Yadav et al., 2020, 2019b; Mishra, Rai and Agrawal, 2013; Fatima et al., 2018).

The main mechanism by which O_3 reduces wheat yields and impacts on quality is through accelerated senescence (Emberson et al., 2018). Wheat cultivars with delayed senescence, stay-green cultivars, have previously been trialled for their potential to offset yield reductions under stressors such as heat and drought stress (Kamal et al., 2019). However, accelerated senescence typically reduces protein remobilisation and reduces wheat quality (Havé et al., 2017; Sultana et al., 2021). Understanding the mechanisms by which O_3 damages crop yield and influences crop quality is crucial for breeding of O_3 tolerant cultivars. Section 2.2.1 provides more detail and a mechanistic description of how wheat yields, and protein, are affected by O_3.

1.3 The current status of crop modelling with regards to N and O_3

Current understanding of the effect of O_3 pollution on wheat nutritional quality has been inferred from experimental studies (Mills et al., 2011; Feng, Kobayashi and Ainsworth, 2008; Broberg et al., 2015, 2021). However, experimental work is time consuming and costly, and it can be difficult to control all variables involved. Crop models use environmental inputs to simulate crop growth, for a range of conditions and stressors, in far less time, using fewer resources than required for experimental investigation (Chenu et al., 2017). Developing crop models with experimental data, which provides insights into plant growth processes, allows investigation of realistic plant responses to individual and multiple stressors.

It is possible to simulate the O_3 effect on grain protein through incorporating N processes into an existing crop model considering O_3 damage, and using a simple conversion factor (e.g. Mariotti, Tomé and Mirand (2008)) to convert N to protein. Many models consider N dynamics in wheat (e.g. APSIM-NWheat and CERES-Wheat) (see supplementary Table S1), and others have incorporated O_3 damage (e.g. LINTULLC2, WOFOST, APSIM and DO_3SE-Crop) (Nguyen et al., 2024; Xu et al., 2023). Some models, such as APSIM, can simulate both O_3 effects on yield and grain N, which could be used to calculate grain protein and hence provide a measure of grain quality variation under O_3 exposure. However, to our knowledge, no simulations have yet been performed on the O_3 effect on grain N. Further, these models do not yet include the mechanisms that relate O_3 with grain N. Currently, no model simulates the reduced remobilisation of N under O_3 exposure from the stem and leaf to the grain, an important determiner of wheat protein under O_3 exposure (Broberg et al., 2021, 2017; Brewster, Fenner and Hayes, 2024; Brewster, 2023; Chang-Espino et al., 2021).

1.4 Objectives

This study aims to develop and use the DO_3SE-Crop model to investigate the impact of O_3 on wheat grain N content through the following objectives:

1) Identifying the key mechanisms necessary to model N in crops and the influence of O_3 on these mechanisms.

95 2) Developing a N module that can be incorporated into the existing O_3 deposition and crop growth model, DO$_3$SE-Crop, to simulate how grain N (and hence protein), is affected by O_3 exposure (DO$_3$SE-CropN).

3) Using the developed DO$_3$SE-CropN model to perform a sensitivity analysis to determine which of the O_3 damage mechanisms (senescence onset, senescence rate/end, and remobilisation of N) affects grain quality the most.

2. Model development

2.1 Overview of the DO$_3$SE-Crop model

100 The DO$_3$SE-Crop model is used to estimate O_3 deposition to a plant canopy and the impacts (biomass and yield loss) caused by stomatal O_3 uptake (Emberson *et al.*, 2018). The crop phenology is estimated based on thermal time sums. Photosynthesis is simulated at the leaf level, based on a modified version of the biochemical Farquhar model (Farquhar, Caemmerer and Berry, 1980), and scaled to the canopy level by splitting the canopy into equally sized layers of cumulative leaf area index (LAI). The

105 photosynthetic products from each layer are summed to give the net primary productivity (NPP). The NPP is allocated to the root, stem, leaf or grain based on the plant's developmental stage using the approach of Osborne et al. (2015). O_3 transfer from the atmosphere to the leaf is estimated by a resistance scheme incorporating aerodynamic, boundary layer and surface resistances above and within the canopy (Pande et al., 2024a). The instantaneous impact of stomatal O_3 flux on photosynthesis and the impacts of accumulated O_3 flux on senescence, once the cumulative flux exceeds a cultivar specific threshold, are

110 estimated based on the approach of Ewert and Porter (2000) and modified by Pande et al. (2024). Further details of the DO$_3$SE-Crop model along with a mathematical description can be found in Pande et al. (2024). In this study version 4.39.11 of the DO$_3$SE-Crop model was used (Bland, 2024).

2.2 Development of the N module

2.2.1 Identification of which N processes to model

115 The key plant processes influenced by N and O_3 were identified to guide decisions on which processes to include in the N module for DO$_3$SE-Crop (Fig. 1). Figure 1 provides an overview of processes already included in DO$_3$SE-Crop, those to be added in the new N module, and those which are excluded. In brief, DO$_3$SE-Crop includes an instantaneous short-term effect of O_3 on carboxylation efficiency which subsequently affects photosynthesis. The leaf has the capacity to recover from this O_3 damage overnight, though recovery ability decreases with age. Additionally, we simulate a long-term effect of O_3 on

120 accelerating senescence. Detail of the DO$_3$SE-Crop model and associated O_3 damage processes are given by Pande et al. (2024a). Figure 1 is separated into numbered sections which are explained in the subsequent text:

#1

Reactive oxygen species (ROS), that are formed when O_3 diffuses through leaf stomata, trigger a series of physiological and

stress responses in the plant that lead to accelerated senescence and a reduced photosynthetic rate (Emberson et al., 2018).

125 ROS delay stomatal response to external stimuli, reducing stomatal conductance (Dai et al., 2019; Paoletti and Grulke, 2010). ROS are detoxified by apoplastic anti-oxidants, but an excess of ROS may overwhelm the anti-oxidant response, damaging cell plasma membrane (Emberson et al., 2018; Fatima et al., 2019).

#2

ROS destroy photosynthetic pigments (Emberson et al., 2018). ROS degradation of photosynthetic pigments accelerates crop

130 senescence, during which Rubisco, comprising 50% of soluble leaf protein, is broken down to release N for remobilization to other parts of the plant (Feller and Fischer, 1994; Emberson et al., 2018).

#3

ROS degradation of Rubisco leads to reduced carboxylation efficiency (Emberson et al., 2018). Together with a reduced electron transport efficiency, photosynthetic rate is reduced (Emberson et al., 2018; Rai and Agrawal, 2012). There is an

135 increase in antioxidant and defence proteins triggered by elevated O_3 (Sarkar et al., 2010; Cho et al., 2011; Fatima et al., 2018).

#4

O_3 induced accelerated senescence reduces the green leaf area for photosynthesis, further decreasing carbon assimilation (Emberson et al., 2018). Diminished photosynthesis leads to lesser photosynthate production (Emberson et al., 2018). More photosynthate is used in respiration and for anti-oxidant production to target ROS (Emberson et al., 2018; Khanna-Chopra,

140 2012). Under O_3 stress, annual crops, such as wheat, prioritise allocation of assimilates to flowers and seeds, reducing the availability for leaves, stems and roots (Emberson et al., 2018).

#5

N taken up by the plant is used to produce all proteins (Lawlor, 2002). Root biomass, and subsequently nutrient uptake, is reduced under stress conditions as assimilate allocation to repair aboveground O_3 damage is prioritised over export to the roots

145 (Emberson et al., 2018; Pandey et al., 2018). While O_3 can induce senescence and reduce photosynthesis, a higher leaf N can delay the onset of senescence and increase the photosynthetic rate (Pilbeam, 2010; Nehe et al., 2020; Martre et al., 2006; Brewster, Fenner and Hayes, 2024). On the other hand, N deficiency can damage the structure and function of the chloroplasts which could exacerbate O_3 impacts on senescence and photosynthetic rate (Kang et al., 2023). Brewster, Fenner and Hayes (2024) found an increase in residual leaf and stem N occurs, potentially as a result of O_3 toxicity.

150 #6

Wheat yields are decreased due to reduced photosynthesis and grain filling duration (Emberson et al., 2018; Broberg et al., 2015). Wheat grain N comprises N taken up post-anthesis, and N remobilised from the leaves and stem when senescence begins (Havé et al., 2017; Gaju et al., 2014; Nehe et al., 2020; Barraclough, Lopez-Bellido and Hawkesford, 2014). Hence, any damage mechanism which affects grain filling duration, influences the final N content of the wheat grains. Additionally,

155 as Rubisco is a key source of N for grains, once senescence begins, reductions to Rubisco will impact the amount of N that is available to grains (Feller and Fischer, 1994). Brewster, Fenner and Hayes (2024) and Chang-Espino et al. (2021) find evidence of an additional, unknown process, separate to accelerated senescence, that reduces the remobilisation of N under O_3 exposure.

Generally, grain protein concentrations increase under elevated O_3, due to a smaller decrease in N uptake and re-translocation relative to the O_3-induced decrease in grain DM (Wang and Frei, 2011; Broberg et al., 2015, 2019; Triboi and Triboi-Blondel,

160 2002; Piikki et al., 2008). However, per metre square of crop the starch and grain protein yield is reduced (Broberg et al., 2015; Feng, Kobayashi and Ainsworth, 2008; Gelang et al., 2000). Some wheat cultivars have shown a decrease in grain protein concentration under O_3 exposure (Yadav et al., 2019a; Baqasi et al., 2018; Mishra, Rai and Agrawal, 2013). This could be because leaf proteins are converted to enzymatic antioxidants to defend against O_3 induced damages, resulting in less proteins available for translocation to the grains (Yadav et al., 2019b; Sarkar et al., 2010; Fatima et al., 2018).

165
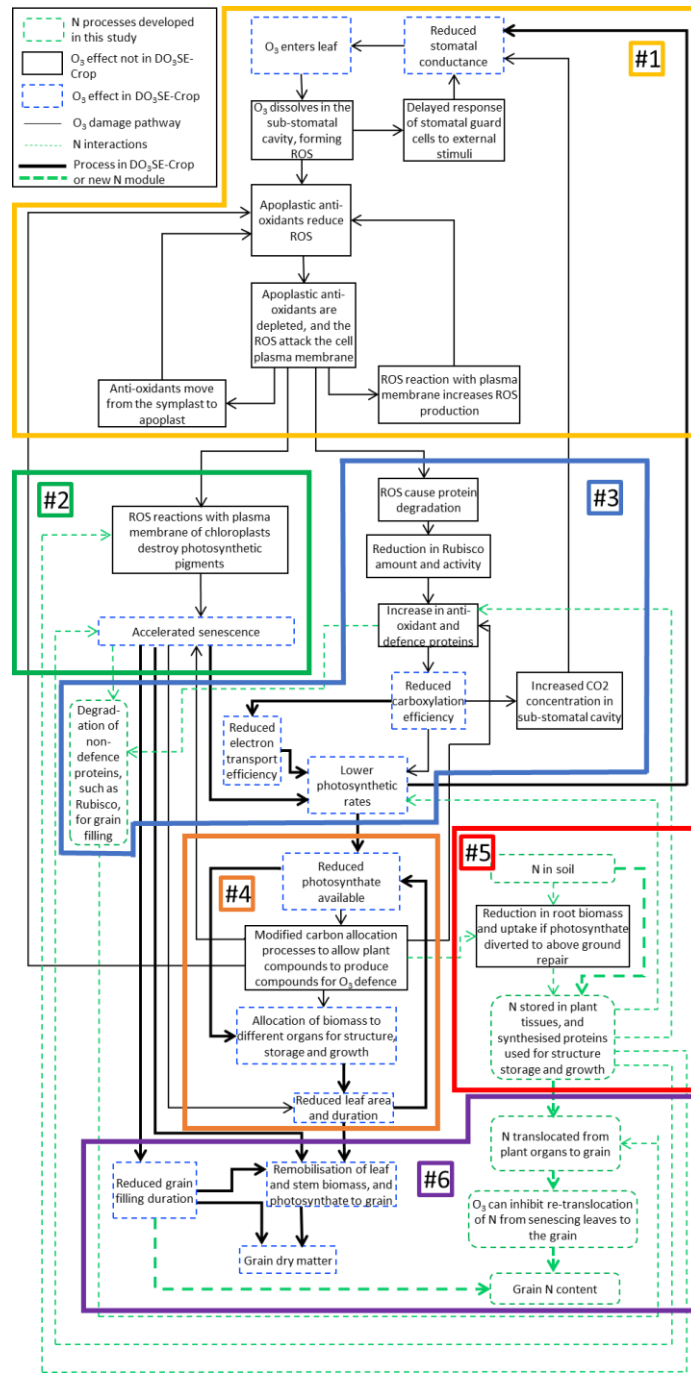
Fig. 1: A flow chart of the mechanisms by which O₃ causes damage to both grain yields and grain N (or protein) in wheat. The different colours and line styles outlining the individual boxes represent whether the process is included in the DO₃SE-Crop model already (blue, dashed outline), not included in the DO₃SE-Crop model (black, solid outline), or included in the N module developed for DO₃SE-Crop in this study (green dashed outline, rounded edge boxes). The black connector lines represent interactions between the O₃ damage processes and the green dashed connector lines represent where N processes interact with these. The thinner lines represent interactions that are not included in the DO₃SE-Crop model or the new N module, whereas thicker lines represent the

interactions that are included. The figure has been divided into 6 numbered sections for which the mechanisms are described individually in Sect. 2.2.1.

2.2.2 Assessment of existing crop models that include N

Supplementary Table S1 summarises and discusses the similarities between models that simulate plant N dynamics. Most models simulated leaf and stem N by fulfilling the required N demanded by the respective parts from the N uptake pool, with N demand based on a defined minimum and maximum for that organ. The maximum and minimum N concentrations can be set as constants or defined using the phenological stage of the plant, which in turn is based on the accumulation of thermal time or a temperature sum based on a scheme by van Keulen and Seligman (1987). Most crop models define a labile pool of N available to be translocated to the grain and consisting of N available from post-anthesis uptake, non-structural stem N, and N released from leaf senescence. The N released from leaf senescence is calculated in proportion to the decrease in carbon of green leaf area, as N remobilisation is proportional to carbon remobilisation (Havé et al., 2017). Most of the crop models simulated grain N by calculating and fulfilling a N demand, or simulating a rate at which the grains fill with N.

2.2.3 Modifications to the existing DO₃SE-Crop model for this study

Prior applications of the DO₃SE-Crop model have assumed that the last 33% of the mature leaf lifespan is when leaf senescence occurs (e.g. Pande et al., 2024). In some of these applications, multiple leaf populations were considered. Given the limitations of available data in parameterising the model for multiple leaf populations, only one leaf population is considered in the present study. As a result, the fraction of mature leaf lifespan that is senescence needed to be modified to instead simulate the fraction of canopy mature leaf lifespan that is senescence. Recent work by Brewster et al. (2024) has shown that the 4th leaves can begin to senesce even before anthesis. Given the importance of senescence in determining N remobilisation (Nehe et al., 2020; Gaju et al., 2014), work by Brewster et al. (2024) was used to re-parameterise the onset of rapid phase senescence as the last 75% of the canopy level mature leaf lifespan for the Skyfall cultivar in DO₃SE-Crop.

2.2.4 The DO₃SE-Crop N module for wheat

Based on Sect. 2.2.1 and 2.2.2, we identified key processes for inclusion in the N module as: soil N uptake, partitioning of N uptake between leaf and stem, remobilisation of N in leaf and stem to the grains, grain filling with N, and O₃ effects on grain N. At the present stage of the modelling, we do not include any processes relating to usage of N for antioxidant production or utilisation of photosynthate for above ground repair due to lack of data for parameterisation. Full details of equations, sources of equations and model parameterisations are available in Appendix A. Briefly:

(a)   Soil N uptake

Pre-anthesis, daily N uptake from the soil is proportional to the increase in LAI and stem mass that day, along with any N deficit that has accumulated over the plant's life, following the work of Soltani and Sinclair (2012). Post-anthesis, we use the formulation from SiriusQuality (Martre et al., 2006) which links post-anthesis N uptake with the capacity of

the stem to store N. Pre- and post-anthesis we define a maximum N uptake which cannot be exceeded. Since we did not have data to calibrate for the effects of N stress, the present model assumes optimal soil N availability.

(b)   N partitioning

Pre-anthesis, N uptake is allocated to the leaf and stem in accordance with the increase in LAI or stem mass that day, as commonly used by other crop modellers (Sect. 2.2.2). The specific equations used closely follow those of Soltani and Sinclair (2012).

(c)   N remobilisation

After anthesis, N remobilisation from the stem to the grains begins. N is released from senescing leaves in accordance with the decrease in LAI that day. Released N is stored in the stem where it is available to the grain. The combination of N released from leaf senescence and non-structural stem N creates the labile pool of N for grain filling.

(d)   Grain N

The N in the labile pool can be transferred to the grain, or it can remain as part of the stem. In contrast to other crop models, the proportion of labile N transferred to the grain each day follows a sigmoid function. The sigmoid was chosen as it uses only two extra parameters (α_N and β_N) which allows the start and rate of grain fill with N to be customised without the addition of much complexity. The fraction leaving the labile pool increases as the plant develops.

$$N_{to\_grain} = N_{labile} \times \frac{1}{1 + exp(-\alpha_N(DVI - \beta_N))} \tag{1}$$

where N_{to_grain} represents the amount of N leaving the labile pool (N_{labile}) to the grains, DVI represents the development index of the plant in DO₃SE-Crop (Pande et al., 2024a). The N_{to_grain} profile for different parameterisations of α_N and β_N is shown in Appendix A, Fig. A3.

(e)   Direct effect of O₃ on grain N

The fraction of N remaining in the leaf and straw increases with O₃ exposure (Broberg et al., 2017, 2021). Additionally, in the work of Brewster et al. (2024) the same effect is observed, where a lower proportion of N stored in these parts at anthesis is moved to the grains. Little data is available on this effect, so we used all available existing data from Broberg et al. (2017) and Brewster et al. (2024) to produce a linear regression of the % of N remaining in the leaf and stem at harvest as a function of M12 (the common metric for the two studies defined as the 12 hour mean O₃ concentration during daylight hours (Guarin et al., 2019)). The results of this can be seen in Fig. 2.
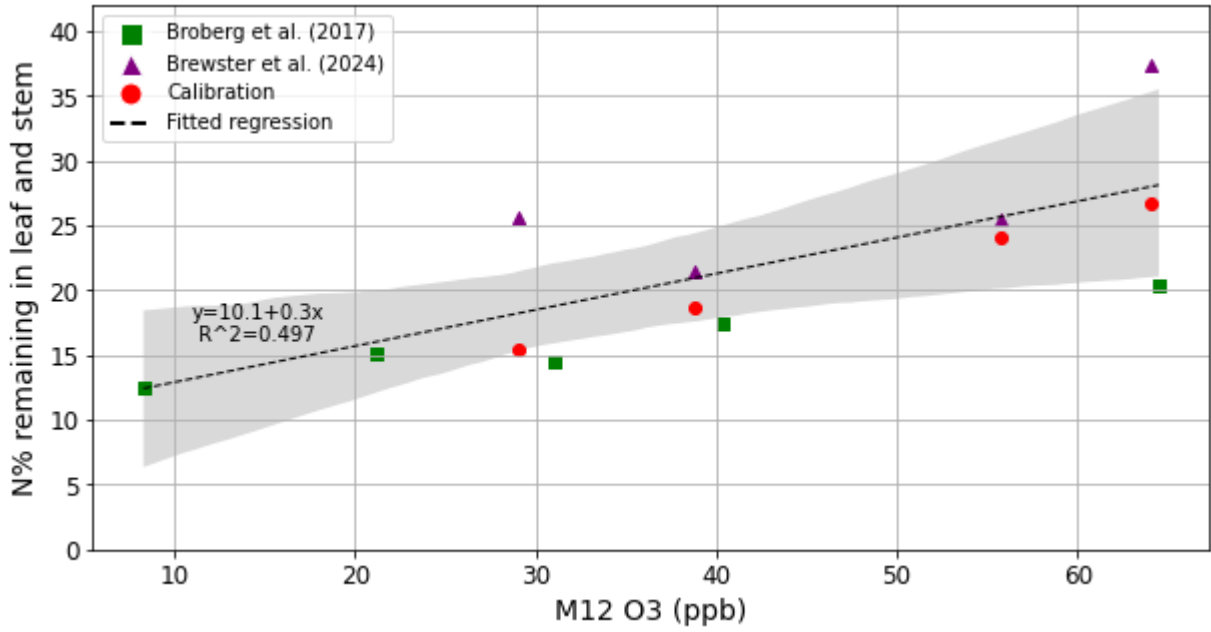
Fig. 2: The % of N remaining in the leaf and stem as a function of M12 for studies by Broberg et al. (2017) (green square markers) and supplementary data obtained from Brewster, Fenner and Hayes (2024) (purple triangular markers). The grey area represents the 95% confidence interval of the fitted regression (dashed linear line) and the R^2 of the regression is given on the figure. Overlaid are red, circular markers showing the effect of the calibrated $m_{leaf}, c_{leaf}, m_{stem}$ and c_{stem} on overall remobilisation.

The minimum allowed leaf and stem N concentrations were varied to optimise the grain N% and harvest leaf and stem N% simulations, whilst making sure the % of N remaining in the leaf and stem was within the 95% CI of the remobilisation regression. The form of the regressions representing the minimum leaf and stem N concentrations under O_3 exposure are given in Eq. (2) and (3) respectively.

$$\frac{[N_{leaf,min}]}{1\ gN\ LAI^{-1}} * 100 = m_{leaf} \times \frac{[O_{3,M12}]}{1\ ppb} + c_{leaf} \tag{2}$$

$$\frac{[N_{stem,min}]}{1\ gN\ DM^{-1}} * 100 = m_{stem} \times \frac{[O_{3,M12}]}{1\ ppb} + c_{stem} \tag{3}$$

where $[N_{leaf,min}]$ is the minimum leaf N concentration in gN per unit of LAI, $[N_{stem,min}]$ is the minimum stem N concentration in gN per g of stem DM, and $[O_{3,M12}]$ is the concentration of O_3 using the M12 metric in ppb. The parameterisation for Eq. (2) and (3) is given in Table 1. Further details of the process by which the best parameters were obtained is given in Sect. 4 of Appendix A.

10

Table 1: The calibrated values for the newly developed regressions describing how the minimum leaf and stem N concentrations vary under differing O$_3$ concentrations. All parameters are unitless.

Parameter	Description	Value
m_{leaf}	Gradient of Eq. (2)	0.8
c_{leaf}	Intercept of Eq. (2)	10.9
m_{stem}	Gradient of Eq. (3)	0.014
c_{stem}	Intercept of Eq. (3)	0.23

(f)   Indirect effect of O$_3$ on grain N

In the DO$_3$SE-Crop model, O$_3$ accelerates the onset and rate of senescence (Pande et al., 2024a). In this N module, remobilisation of N from senescing leaves occurs once senescence begins. Further, no N is remobilised from the leaves once senescence is complete. DO$_3$SE-Crop also simulates the impact of O$_3$ on the rate of photosynthesis and, consequently, biomass production and leaf area expansion (Pande et al., 2024a). In this N module, leaf area determines accumulation of leaf N and stem biomass determines accumulation of stem N, providing an indirect link between O$_3$ damage in the DO$_3$SE-Crop model and the newly developed N module.

In combination, the N and DO$_3$SE-Crop processes are integrated to form the DO$_3$SE-CropN model as shown in Fig. 3. Simply, N uptake is partitioned in accordance with demand from the leaf and stem. The N available to the grain comes from senesced leaf area, post anthesis N uptake and non-structural stem N. The amount of N that is transferred to the grain from this available pool is calculated using a sigmoid function. The fraction of N that is available to the grain from the leaf and stem is modified in accordance with daily O$_3$ concentrations. Further details of the equations used, and processes involved are given in Appendix A. In this study version 1.0 of the N module was used, and the corresponding code can be found at Cook (2024).
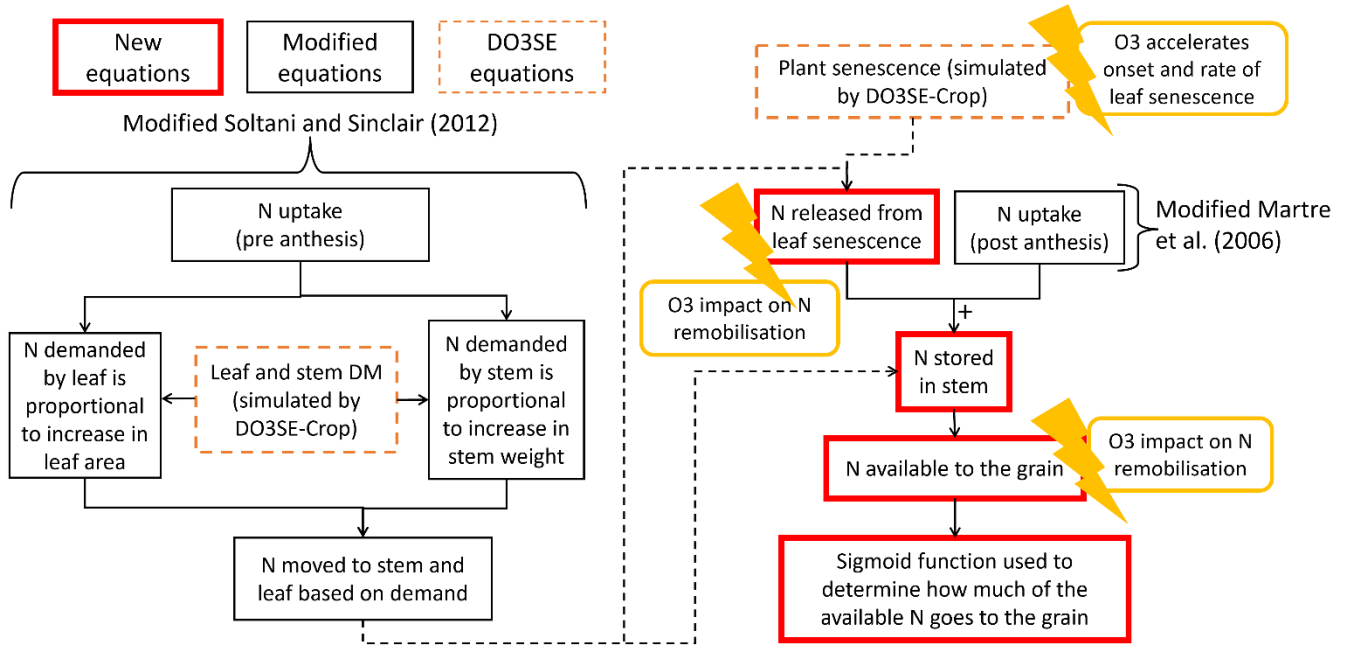
Fig. 3: Simplified overview of the DO₃SE-Crop N module. Red outlined boxes show the processes developed in this study. Orange outlined boxes are indicating where the N module takes outputs from the DO₃SE-Crop model. Black outlined boxes indicate where equations were taken from the existing literature and modified for the current study. The lightning bolts represent the locations where O₃ impacts on plant N processes in the newly developed DO₃SE-CropN model.

3. Parameterisation and calibration of DO₃SE-Crop and new N module

Experimental data have been collated and gap filled (using the AgMIP-Ozone gap-filling methodology (Emberson et al., 2021)) to calibrate and evaluate the DO₃SE-Crop model and newly developed N module. Further details of the gap filling methods can be found in the Supplementary materials.

3.1 Experimental datasets

Data from the Centre for Ecology and Hydrology, Bangor, from the years 2015, 2016 and 2021 were used to calibrate the N module for DO₃SE-Crop. For each year, the Skyfall wheat cultivar was grown in solar domes under 4 O₃ treatments, with median O₃ concentrations ranging from 29 – 61.1 ppb. Across the 3 years, the wheat was planted between February 23rd and April 15th and harvested between August 11th – August 17th. O₃ fumigation occurred between stem-elongation (GS30) and harvest (mid-August) (Brewster, Fenner and Hayes, 2024; Broberg et al., 2023; Osborne et al., 2019 with supplementary information from the authors). In this study, only treatments where the plants were well watered and experienced no N or temperature stress were used. No grain data was used for the year 2021 as the plants did not put on any grain (see Brewster, Fenner and Hayes (2024) for further detail). A tabulation of data available from each year can be found in supplementary Table S2. Further details of the experimental set up for all years can be found in Brewster et al. (2024), Broberg et al. (2023) and

Osborne et al. (2019) and supplementary data obtained from the authors was used for model development (see data availability).

3.2 Model calibration and evaluation

Model calibration was performed in stages, with the calibrated parameters indicated in brackets. Definitions of DO$_3$SE-Crop parameters, along with the value they were calibrated to and the units are given in supplementary Table S3.

1) Phenology ($T_b, T_o, T_m, TT_{emr}, TT_{flag,emr}, TT_{astart}, TT_{amid}, TT_{harv}$)

2) Photosynthesis and respiration ($V_{cmax,25}, kN, J_{max,25}, m, R_{dcoeff}, R_g$)

3) DM allocation and yield, and O$_3$ effect on yield and senescence ($\alpha_{root}, \beta_{root}, \alpha_{leaf}, \beta_{leaf}, \alpha_{stem}, \beta_{stem}, \Omega, \tau, E_g, \gamma 3, \gamma 4, \gamma 5, CLsO3$)

4) N allocation and O$_3$ effect on N remobilisation ($m_{leaf}, c_{leaf}, m_{stem}, c_{stem}$ (Sect. 2.2.4, Table 1))

This sequential calibration prevents later adjustments caused by the interdependencies between parameters at different calibration stages. It was necessary to calibrate O$_3$ effects on yield at the same time as the DM allocation and yield parameters, as O$_3$ still influences yield, even in the low O$_3$ treatments. $V_{cmax,25}$ and $J_{max,25}$, had been measured and so were fixed to their experimentally measured values to limit the numbers of parameters to calibrate. Further, data on photosynthesis at different light concentrations allowed the determination of the rate of dark respiration, and hence we fixed the parameter controlling dark respiration in DO$_3$SE-Crop. A combination of genetic algorithm and manual calibration was then used to calibrate chosen parameters to achieve the desired output variable. The genetic algorithm is not always the most suitable for model calibration, as it can give parameterisations that maximise the R^2, but don't make sense physiologically. In cases where unrealistic parameterisations were given, a manual "by-eye" calibration process was also used. By varying one parameter at a time to understand it's effect on a desired output, realistic parameterisations were chosen. For all calibrations the R^2 and RMSE were used to assess the fit between observed data and simulations. Generally, 50% of the combined data for all years, for the low and very high O$_3$ treatments were used in the calibration, with the remaining data used in the evaluation along with 100% of the medium and high O$_3$ treatment data for all years. A tabulation of the parameters calibrated for, and the values they were calibrated to, are given in supplementary Table S3 along with further details of the calibration process. Parameterisations relating to the newly developed N module are discussed and presented along with their equations in Appendix A.

The model was evaluated by calculating the RMSE and R^2 of the linear regression between observed and simulated values of phenology dates, grain DM, stem and leaf N and grain N%. More emphasis is placed on the relative O$_3$ impact on yield and quality than simulations of absolute values, as the aim of the study was to develop a model that can capture relative O$_3$ impacts on crop quality.

3.3 Sensitivity analysis

Sensitivity analyses are used to determine the proportion of variance in a desired model output attributed to a variation in the
310 model input (Saltelli et al., 2008). In this study, we use a sensitivity analysis to identify and rank the sensitivity of grain N to different plant processes simulated by DO$_3$SE-Crop and the new N module. We identified 3 key mechanisms that can influence grain quality in the crop model: senescence onset, the end/ duration of senescence and the O$_3$ interruption of N remobilisation of the leaf and stem. A preliminary sensitivity analysis was conducted to identify the key parameters in DO$_3$SE-Crop influencing these processes. After reduction, 4 parameters which contribute the greatest to the variance of output variables
315 representing these processes were identified for the sensitivity analysis (see Table 2). We use an extended Fourier amplitude sensitivity analysis (eFAST) to explain the variation in a chosen output variable attributed to varying selected input variables over a given range (Saltelli et al., 2008). The eFAST method is a commonly used method for sensitivity analyses and has previously been used by crop modellers to improve calibration (Silvestro et al., 2017; Vazquez-Cruz et al., 2014). The benefit of eFAST over other forms of sensitivity analysis is that it allows the interactions between model parameters to be quantified,
320 it can sample the entire parameter space, and it is robust for non-linear relationships (Saltelli et al., 2008; Cariboni et al., 2007). These benefits make it a useful tool for complex systems such as crop models, where interacting, non-linear processes are common (Saltelli et al., 2008; Cariboni et al., 2007). The Python library SaLIB was used for all sensitivity analyses (Herman and Usher, 2019). The first sensitivity index, S1, quantifies the uncertainty in the output variable that is attributed to varying only that parameter. The total sensitivity index, ST, quantifies the uncertainty in the output variable that is attributed to varying
325 a chosen parameter in combination with the other selected parameters (Saltelli et al., 2008). The range of values for the sensitivity analysis were taken from the theoretical maximum and minimum in the DO$_3$SE-Crop model for those mathematical equations. The ranges for $\gamma 4$ and $\gamma 5$ were determined using the breakpoint method, as described by Pande et al. (2024b). For the leaf and stem remobilisation equations, the minimum gradient is 0 as this assumes no O$_3$ effect on remobilisation for that plant part, and the maximum gradient was calculated by assuming that the other plant part has had as close to zero O$_3$ impact
330 on remobilisation as is mathematically possible in the equation formulation.

335

Table 2: The parameters included in the sensitivity analysis along with a specification of the values for the ranges between which they were varied in during the analysis

Parameter	Unit	Explanation	Minimum	Maximum
$\gamma 4$	-	O_3 long-term damage co-efficient determining onset of senescence	0.1	10
$\gamma 5$	-	O_3 long-term damage co-efficient determining maturity	0.1	1.5
m_{leaf}	-	Gradient of regression determining minimum leaf N concentration under O_3 exposure (influences how much leaf N is available for remobilisation)	0	3.024
m_{stem}	-	Gradient of regression determining minimum stem N concentration under O_3 exposure (influences how much stem N is available for remobilisation)	0	0.0312

4. Results

4.1 End of season grain DM and N% in grain, leaf and stem

Figure 4 shows the evaluation of the grain DM, and grain, leaf and stem N% simulations. Leaf and stem N data were only available in 2021, hence the leaf and stem plots only use data from 2021. Additionally, for 2021, the plant did not put on any grain (the reason for which is unknown (Brewster, Fenner and Hayes, 2024)) which meant it was not possible to use the grain DM or grain N data for that year. However, since this was the only year of data for which stem and leaf N% measurements were available and the plants developed and flowered normally, the decision was made to proceed with these data for stem and leaf parameterisation. For 2016, the model captured the grain DM and the grain N% more precisely than for the year 2015. In 2015, the under-estimate of grain DM resulted in an overestimation of grain N%. The stem and leaf N% at anthesis is better simulated than at harvest. Harvest leaf N is overestimated by between 20-120%, while harvest stem N overestimations range from ~40-120%. However, in both the stem and the leaf, N concentrations are over-estimated at both anthesis and harvest, despite the calibration showing the remobilisation of N from the leaf and stem under the differing O_3 concentrations was well

captured (see Fig. 2). The R^2 values (calculated using scikit Learn, developed by Pedregosa et al. (2011)) for grain DM and grain N% are negative, implying that the model simulations are worse than using the mean of the observed data (scikit-learn developers, 2023).
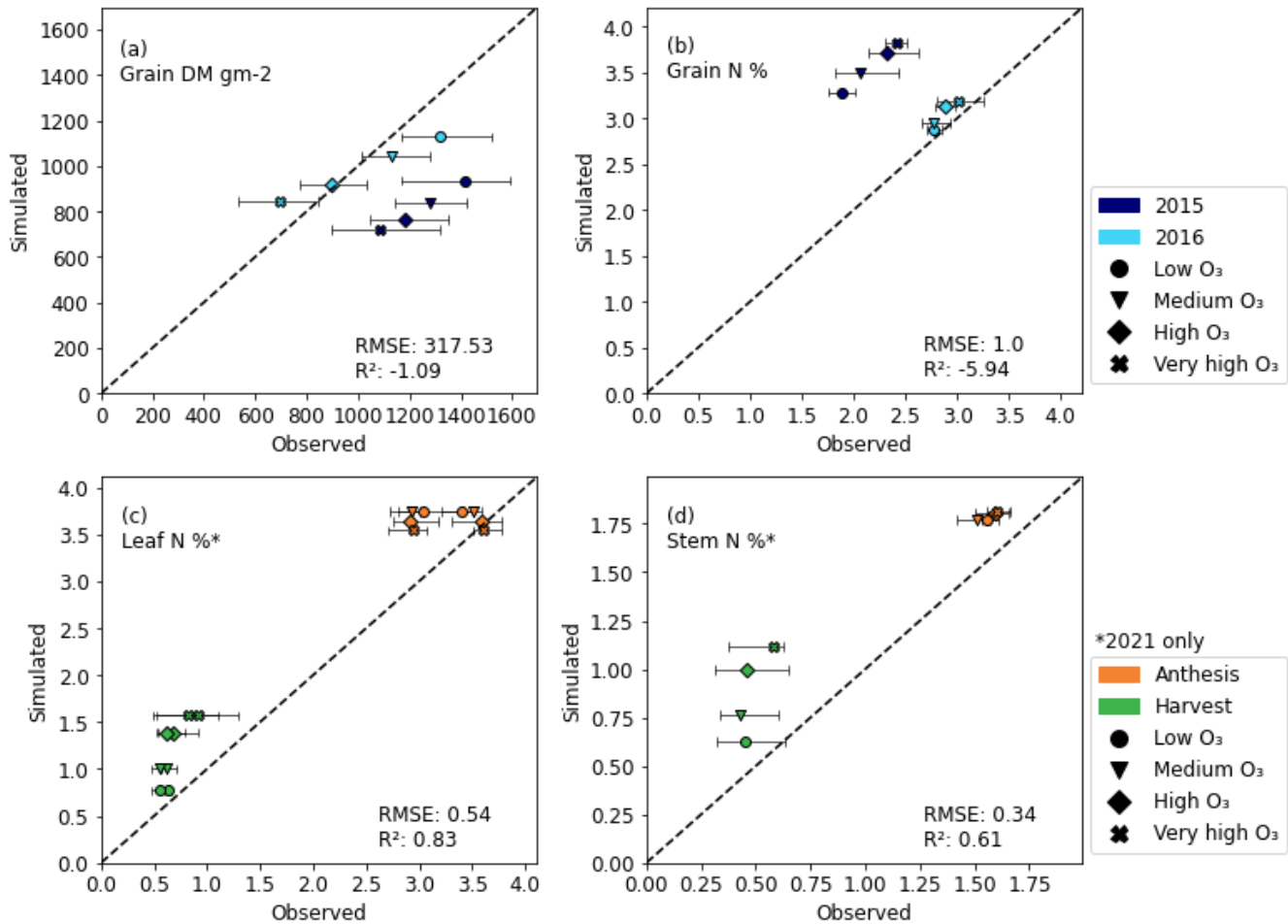

Fig. 4: Output of the DO₃SE-Crop grain dry matter simulations at harvest (a), and the newly developed N module simulations of grain N% at harvest (b), leaf N% at anthesis and harvest (c), and stem N% at anthesis and harvest (d). The simulations shown are for the evaluation datasets only. The evaluation data available contained grain dry matter and N% for 2015 and 2016, whereas for 2021 the plant did not put on any grain, so this data was not used for evaluation. Leaf and stem N% data was only available for 2021. The RMSE and R^2 of the observed versus simulated data (not including error bars) are shown on the plots. The error bars represent the maximum and minimum of the experimental data, excluding outliers, for comparison with simulations. The leaf N% figure contains data for both the flag and 2nd leaf. DO₃SE-Crop and the new N module do not discriminate between these so simulations of leaf N% for flag and 2nd leaf are the same

The relative yield (RY) loss of the 2015 simulations is much better simulated than the 2016 simulations (Fig. 5). However, the R^2 is 0, meaning that the simulations work equally well as when using the mean of the observed data (scikit-learn developers, 2023). When considering grain quality, the increase in grain N% that occurs as O_3 concentrations increase, is simulated very effectively with an R^2 of 0.6 and a RMSE of 4.9%. The % decrease in grain N content (grain N content measured in grams of

N per m^2 of crop) is not simulated as well as the change in grain N concentration, as is seen from the lower R^2 (0.3) and greater RMSE (14.4). Further, Fig. 5c shows that the model had trouble capturing the large differences in grain N content that occurred in 2016, compared to the much smaller differences in 2015.
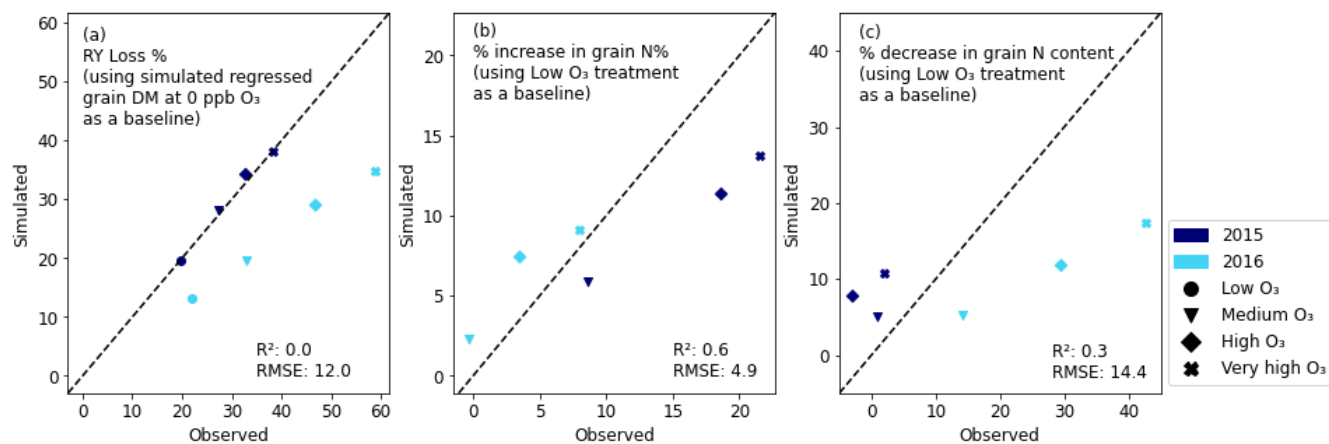
370

Fig. 5: Relative plots of the evaluation data. (a) the relative yield (RY) loss of the grain DM when using the grain DM at 0 ppb (obtained by regressing the simulated and observed yields) as a baseline. (b) the % increase in grain N% and (c) the % decrease in grain N content (gm^{-2}) when using the low O$_3$ treatment as a baseline. The RMSE and R^2 of the observed versus simulated data (not including error bars) are shown on the plots.

375 **4.2 Seasonal profiles of grain DM, grain N content and N% in the grain, leaf and stem**

The profile of grain DM accumulation over time for all treatments is shown in Fig. 6 for 2015 and 2016, and for all years in Fig. S5. From the profiles we see that initially accumulation of grain DM is slow, then at days 200 and 192 for 2015 and 2016 respectively, there is a rapid increase. From the plots we can see the O$_3$ effect on grain DM accumulation begins around 5-10 days post-anthesis.

17
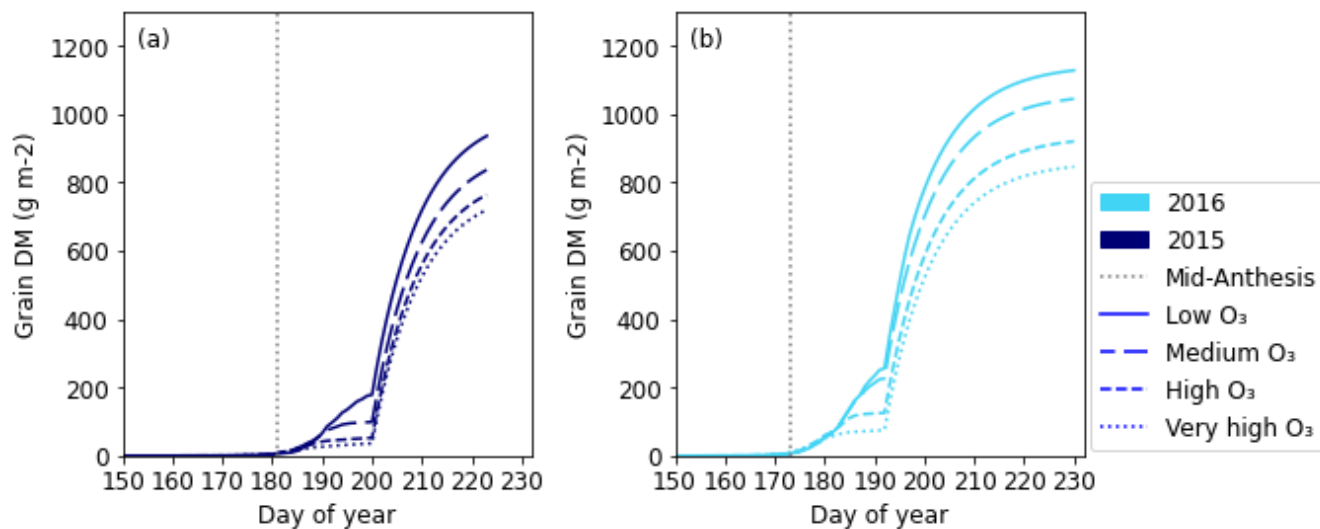
380

Fig. 6: The profile of simulated grain DM for 2015 (a) and 2016 (b). Mid-anthesis is indicated on the graph as a vertical dotted line and the different line styles on the plot represent the simulations for the different O_3 concentrations.

Figure 7 shows the change in simulated grain N% and grain N content as a function of time under the different O_3 concentrations. As O_3 concentrations increase, the absolute grain N content in gm^{-2} (Fig.'s 7c and 7d) decreases for both years.

385 Figures 7a and 7b appear to show a very sharp increase in grain N% as the grain starts filling with N after anthesis, and then after approximatley 20 days N concentration starts to decrease. This rapid increase is due to a difference in the accumulation rates of grain DM and N in the model, and is not representative of a plant process (see Supplementary Fig. S1). Due to the large spike in initial N concentrations, it is difficult to see the effect of O_3 on the end N concentrations. Therefore, the end profiles of the grain N concentrations were enlarged in Fig.'s 7a* and 7b*. Once magnified, it is possible to see the increase

390 in grain N% with increasing O_3 concentrations.
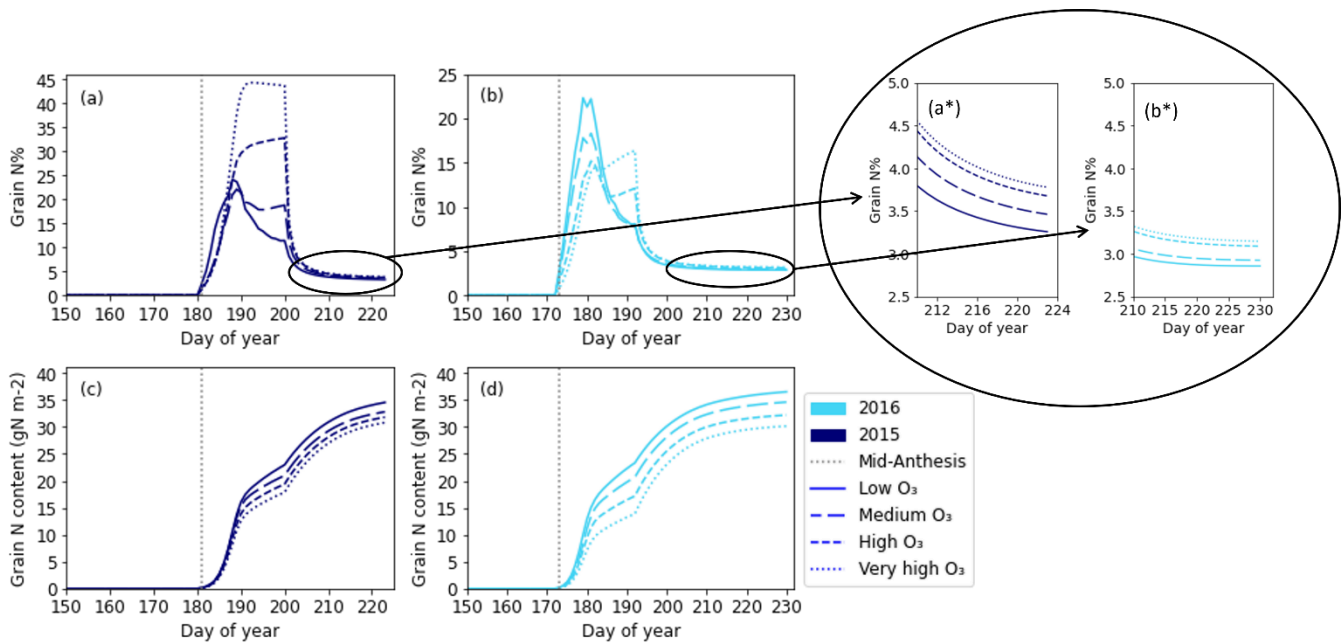
Fig. 7: The simulated grain N% for 2015 (a), and 2016 (b), and the simulated grain N content in grams per metre squared for 2015 (c) and 2016 (d). The different line styles represent the different O_3 concentrations. Mid anthesis is indicated on the graph as a dashed vertical line for each year. The end points of figures (a) and (b) have been enlarged and are represented as figures (a*) and (b*) respectively so that differences at the end points can be distinguished.

Figure 8 shows the seasonal profile of leaf and stem N content and % under differing O_3 concentrations. Simulations of leaf and stem N% (Fig.'s 8a and 8b) are relatively constant at their target N concentration (see Appendix A for target N explanation), until anthesis, since the model assumes no limitations to soil N uptake. The leaf and stem N content increase in line with increasing biomass. Post-anthesis, the stem begins to transfer N to the grain, and so the N concentration and content in the stem decreases (Fig.'s 8b and 8d). The remobilisation of N from the stem to the grain continues provided the stem N concentration does not decrease below the minimum (Fig.'s 8b and 8d). The levelling off of the stem N% in Fig. 8b shows the minimum stem N concentration for that O_3 treatment has been reached. At higher O_3 concentrations the stem remobilises less N to the grains and the final concentration of N in the stem is greater (Fig.'s 8b and 8d). Initially leaf N% and content decreases faster in the simulated wheat plants experiencing greater O_3 concentrations, as senescence begins earlier in these treatments (Fig's 8a and 8c). Then, at around 20 days after mid-anthesis the O_3 effect on remobilisation takes over, and the leaf N% and content are greater under increased O_3 concentrations, due to the O_3 inhibition of N remobilisation.

19
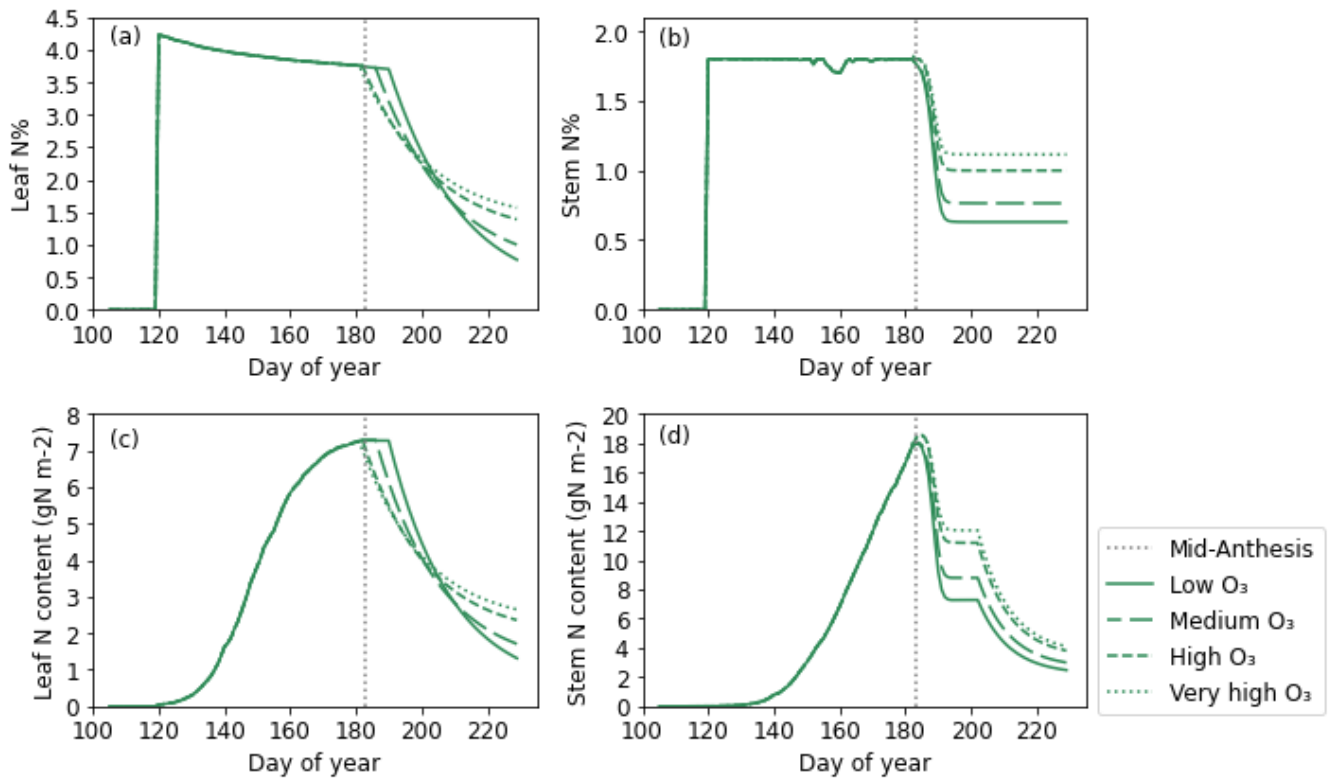
Fig. 8: The simulated leaf (a) and stem (b) N%'s along with the simulated absolute N content in grams per metre squared for the leaf (c) and stem (d). Mid-anthesis is indicated on the graph as a vertical dotted line and the different line styles on the plot represent the simulations for the different O₃ concentrations. These plots are for the 2021 simulations only.

4.3 Sensitivity analysis results

Figures 9a and 9b illustrate the results of the sensitivity analysis study, and show that greater than 60% of the variance in both grain N content and grain N% in simulations of all O₃ treatments is explained by varying the parameter controlling the onset of leaf senescence. Absolute grain N content (gm^{-2}) is more sensitive to variations in senescence onset than grain N%, and grain N% is more sensitive to variations in senescence-end than grain N content. A threshold of $ST > 0.1$ was used by Silvestro et al. (2017) to identify influential parameters in their sensitivity analysis. In this study, senescence onset and senescence end were found to be the only influential parameters on grain N content and grain N%. The effect of varying the leaf and stem remobilisation accounts for less than 2% of the variance in both grain N% and grain N content for all O₃ simulations and can be considered non-influential. The interactions between the parameters were close to zero for the grain N%, as shown by a small difference between S1 and ST. Whereas a stronger interaction was seen when considering absolute grain N as the output. The negligible ST terms for leaf and stem remobilisation imply that the larger ST observed for senescence onset in Figure 9a must be due to the interaction between senescence onset and end. Onset of leaf senescence was simulated as occurring 15, 11 and 12 days earlier in the very high versus low treatments for 2015, 2016 and 2021 respectively.

20
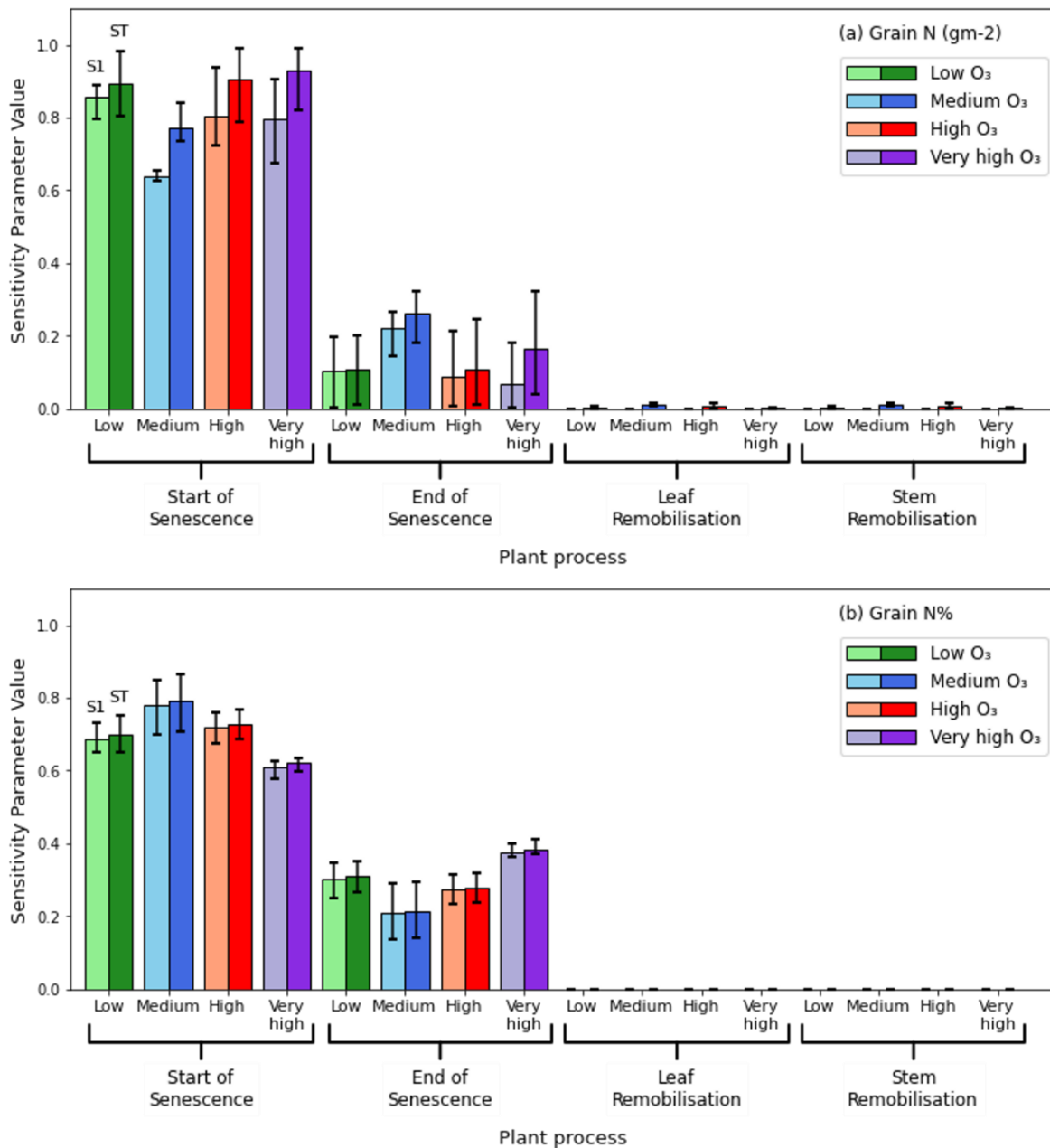
Fig. 9: Results of the sensitivity analysis. Lighter bars represent the first sensitivity index, S1, and the darker bars represent the total sensitivity index, ST. The different colours represent the different O₃ treatments and for clarity are also indicated on the x ticks. Braces group together the results of the sensitivity analysis for a particular plant process. The single model parameter chosen to represent each plant process in this analysis is described in Sect. 3.3. This graph shows the averaged results for the 3 different years. The coloured bars represent the mean value of the sensitivity index for all 3 years, while the error bars represent the maximum and minimum values for that sensitivity index achieved in the runs for the 3 years. Figure (a) shows the results of the sensitivity analysis when considering the absolute grain N content in gN m^{-2} as the output parameter. Figure (b) shows the results of the sensitivity analysis when considering the percentage of N in the grain as the output parameter ($100*gN\ gDM^{-1}$)

5. Discussion

5.1 Evaluation of grain DM simulations

5.1.1 Grain DM simulations at harvest

The relative yield (RY) loss of the wheat in 2015 was more accurately simulated than in 2016, despite the grain DM being better simulated in 2016 than 2015 (Fig.'s 4a and 5a). The variability of whether grain DM or RY loss is better simulated occurs because it is not possible to calibrate grain DM independently of the O_3 effect on yield loss, due to overnight O_3 concentrations of >20 ppb in the solar domes, which give a pollutant effect on yield even in the lowest O_3 treatment. Subsequently, there is a trade-off between achieving a greater accuracy in either grain DM or RY loss simulations as the current model construct was not able to capture both at the same time. In this study, the decision was made to give priority to greater accuracy on the relative O_3 effect on yield, so that we could better test our simulations of the relative effect of O_3 on grain quality. Further, the splitting of data for calibration and evaluation was randomised. The randomisation resulted in the calibration simulations for 2015 having a slightly lower grain DM, and hence the grain DM for 2015 in the evaluation simulations was underestimated.

5.1.2 Seasonal profile of grain DM accumulation

Grain DM accumulation profiles follow an approximate sigmoid shape, with a "bump" in the grain DM profile occurring when the stem begins to allocate DM to the grain (Fig.'s 6a, 6b and S5). Under higher O_3 concentrations, grain DM is reduced ~5-10 days after mid-anthesis. While profiles of grain DM accumulation have not yet been studied for O_3, they have been studied for other stressors such as drought. Given that both drought stress and O_3 damage are ROS mediated we can expect their effects on the seasonal profiles of DM and N to be similar, where the stresses occur continuously throughout the growing season (Khanna-Chopra, 2012; Emberson et al., 2018). Liu et al. (2020) found that drought-stressed wheat initially had a higher grain weight than well-watered wheat 7 days after anthesis, but by 28 days the well-watered wheat had surpassed the drought stressed wheat in weight. Similarly, Zhang et al. (2015) found the grain weight of drought-stressed wheat was higher 12-20 days after anthesis, but by 36 days had been surpassed by the well-watered wheat. In maize, Guo et al. (2021) found a decrease in kernel fresh weight under drought stress 10 days after anthesis, with the effect consistent to the end of the study, as in the present grain DM profiles for wheat. However, Liu et al. (2020) and Zhang et al. (2015) who did study wheat, did not observe a consistently lower grain DM for the drought-stressed wheat as observed in this study (Fig. 6). However, their profiles were based on individual grains (Liu et al., 2020) and the thousand grain weight of the 4 main spikes (Zhang et al., 2015). Neither of those values take into consideration the reduced number of grains per plant that occurs under drought stress (Mariem et al., 2021). Reduced grain numbers are also observed under O_3 stress (Broberg et al., 2015). Therefore, a consistently lower grain DM profile when presented as a grain DM per metre squared (as in this study) may be expected for increasing levels of stress. Together, these data suggest that differences in grain DM accumulation under drought stress are evident as early as 7-10 days post-anthesis. Therefore, it is not unreasonable that our simulations to show a decrease in grain DM accumulation in O_3 exposed

22

465 wheat 5-10 days after mid-anthesis. Further, considering the grain DM per metre squared, we may expect to see a consistently lower grain DM for plants experiencing greater O_3 stress.

5.2 Evaluation of grain N simulations

5.2.1 Grain N simulations at harvest

Harvest grain N% is simulated well for 2016, when the grain DM is more closely captured (Fig.'s 4a and 4b). However, in 2015, when the grain DM is under-estimated, the grain N% is over-estimated. The over-estimation of grain N% is reduced when the observed, rather than simulated, grain DM values are used to calculate grain N% (data not shown). This suggests that the newly developed N module can simulate the absolute grain N% under differing O_3 treatments accurately, provided grain DM is simulated well.

The model captured the increase in grain N% ($100*gN\ gDM^{-1}$) under elevated O_3 much better than the decrease in grain N content (gN m-2) (Fig.'s 5b and 5c). The model was calibrated to grain N% as the response of grain N% to O_3 was more consistent between years than grain N content. Between the two years of data there were large differences in the grain N content of the wheat at harvest, the reason for which is unclear, though it could partially be due to the differences in grain DM between the two years. Since the grain N content was so different between the 2015 and 2016 datasets for all treatments, the model struggled to match both years when simulating the decrease in grain N content. Additionally, the interdependence between grain DM and N meant that in the calibration, changing one of them subsequently changes grain N%, making the calibration process more difficult (see supplementary Fig. S1). If the wheat in 2021 had put on grain, the grain N measurements would have been invaluable in determining which of 2015 and 2016 had the more common response of grain N to O_3 for the Skyfall cultivar. Having at least 3 datasets for model calibration allows outliers to be more easily identified, and more physiologically representative data selected for calibration.

5.2.2 Seasonal profile of grain N accumulation

The seasonal grain N content profiles (Fig.'s 7c and 7d) match well with profiles seen in experimental work (Nagarajan et al., 1999; Bertheloot et al., 2008) and that can be constructed from available wheat N data (see supplementary Fig. S2). There is a "bump" in our simulated grain N content (Fig.'s 7c and 7d) which matches that of our simulated grain DM profile (Fig.'s 6a and 6b). The "bump" occurs because as stem DM decreases (due to remobilisation), it increases the available N for the grain. It is not thought that this "bump" represents the actual rate by which the grain fills with N, but instead occurs due to the complex interconnections between leaf senescence, leaf N remobilisation, stem N remobilisation and required N for the grains in the model.

The seasonal profiles of grain N content (Fig.'s 7c and 7d) show that O_3 effects are distinguishable ~10 days after mid-anthesis, with the model simulating lower rates of accumulation of grain N content when wheat is exposed to higher concentrations of 495 O_3. To our knowledge, no studies describe how the seasonal profile of grain N content accumulation varies under differing O_3

concentrations. However, again using that both O_3 and water stress are ROS mediated (Khanna-Chopra, 2012; Emberson et al., 2018), the response of grain N accumulation under water stress, compared to a well-watered treatment, could be comparable to grain N accumulation under different O_3 concentrations. Nagarajan et al. (1999) found varying responses in grain N accumulation between cultivars for water-stressed wheat, with some showing similar profiles to the control treatment and others experiencing a negative impact on both total N and rate of accumulation compared to the control.

In a study measuring N accumulation with and without irrigation, Panozzo and Eagles (1999) found that the irrigated wheat accumulated N more slowly per grain, but continued accumulating for longer and ultimately had a higher N content per grain. In the current study, our simulations show that the grains accumulated less N content under O_3, which occurs due to the explicit modelling of a reduced remobilisation rate under higher O_3 concentrations (Fig.'s 7c and 7d and Eq. (2) and (3)).

Seasonal profiles of grain N% (Fig.'s 7a and 7b) under different O_3 treatments are less consistent than the grain N content profiles. Initially, grain N% increases rapidly, then levels-off and decreases. Using data from Nagarajan et al. (1999) who measured grain N and carbon (C) of wheat cultivars at 3 time points post-anthesis under water stress and control conditions, we constructed time profiles of grain N% (see supplementary materials and Fig. S4). The constructed profiles generally show an initial increase in grain N% which tends to decrease or level-off, as in the present study. Panozzo and Eagles (1999) measured grain weight and N for 7 time points post-anthesis, again allowing a profile of grain N% under dry and irrigated treatments to be constructed. The profiles show that the wheat grain N% decreases from 2.5% and levels off to 2% approximately 21 days after anthesis, matching the shape of our grain N% profile, though our peak grain N% is far too large at 15-45% (Panozzo and Eagles, 1999). In our study, the reason for the large peak in grain N% is that N accumulation occurs more rapidly after anthesis than grain DM, leading to a greater concentration of grain N (see supplementary Fig. S1). If the initial rate of grain fill with N was slower, or grain DM accumulation was faster, our grain N% profiles would likely match the shape and magnitude of those constructed from Panozzo and Eagles (1999) or Nagarajan et al. (1999). It would be helpful to have measurements of grain N content and DM for multiple time points after anthesis under varying O_3 treatments, to develop a temporal understanding of grain N% response to O_3 for model parameterisation.

In 2015, grain N% is already higher in the elevated O_3 treatments around 10 days after anthesis, whereas in 2016 grain N% is initially higher in the lower O_3 treatments and then around 20 days after mid-anthesis, the elevated O_3 show a higher grain N% (Fig.'s 7a and 7b). The difference in response of grain N% is due to the differences in the simulated rates of grain N and grain DM accumulation between the years. In the grain N% profiles constructed from Panozzo and Eagles (1999) (see supplementary Fig. S3), the irrigated (non-stressed) wheat had a lower final grain N% than the dry (stressed) treatment and the difference was clear to see from > 10 days post-anthesis. Toward harvest, the effect of increased O_3 concentrations on increasing the grain N% is seen approximately 20 days after anthesis, when the initial sharp increase levels off and the concentrations reach more reasonable values.

5.3 Evaluation of stem and leaf N simulations

5.3.1 Stem and leaf N simulations at anthesis and harvest

The anthesis leaf and stem N% are captured well by the model but the effect of O_3 on harvest leaf and stem N% is exaggerated
530 Fig.'s 4c and 4d). Although the differences between harvest leaf and stem N% were non-significant (Brewster, Fenner and Hayes, 2024), there appears to be a slight decrease in final leaf and stem N% under the medium O_3 treatment and a subsequent increase for the high and very high O_3 concentrations. A potential reason for the decrease under medium O_3 concentrations could be an effect called hormesis, where a stressor initially induces a greater productivity in the plant and then, past a given threshold, has a negative effect (Agathokleous, Kitao and Calabrese, 2019). While it could be argued that hormesis is present
535 for the data of Brewster, Fenner and Hayes (2024) in Fig. 2 of this study, there are only 4 O_3 treatments which means it is not possible to parameterise the minimum point of the hormetic response. Whereas Broberg et al. (2017) had 5 O_3 treatments, yet did not observe a hormetic response, and instead found it linear. If future experimental work looks at the O_3 impact on N remobilisation from the leaf and stem to the grain, it would be helpful to place a greater emphasis on O_3 treatments between 30-60 ppb to determine a potential turning point at which higher O_3 concentrations start to limit N remobilisation. This would
540 enable parameterisation of a non-linear hormetic response for N remobilisation in wheat under O_3 exposure.

5.3.2 Seasonal profiles of stem and leaf N accumulation

Our simulations of leaf and stem N content and N% over time (Fig. 8) show that they reach a peak before anthesis and decrease after anthesis, which is also shown by the stem and leaf N profiles constructed from available experimental data (see supplementary Fig. S2). The levelling-off of the stem N content (Fig. 8d) profile at approximately 190 days is a result of the
545 model construct in that no N was required for the grains from the stem at that point.

Currently, there are no data in the literature describing the effect of O_3 on leaf or stem N status in crop plants over the course of the growing season to compare with the present study (Fig. 8). However, one study by Bielenberg, Lynch and Pell (2002) did measure the variation in stem and leaf N content, over time, in hybrid poplar exposed to elevated O_3. In plants receiving the same N treatment, increased O_3 generally reduced the N content of the leaves and stem at each measurement point.
550 Generally, the temporal profiles of N content had the same shape regardless of O_3 treatment (Bielenberg, Lynch and Pell, 2002). In our study, the stem N content was greater at every stage post-anthesis for greater O_3 concentrations due to the reduced remobilisation of nutrients under O_3 exposure (Brewster, Fenner and Hayes, 2024). By contrast, the leaf N content was initially reduced in wheat experiencing greater O_3 concentrations due to accelerated senescence, but the effect of the reduced remobilisation eventually outweighed the senescence effect, leading to greater N content in O_3 stressed wheat at harvest.

555 ### 5.4 Suggestions for improving the representation of plant growth in DO₃SE-CropN

It has been suggested that the reduced remobilisation of leaf and stem N under O_3 exposure occurs as a result of reduced N use efficiency, as O_3 accelerated senescence shortens the grain filling period (Broberg et al., 2021, 2017). However, Brewster et

al. (2024) found an increase in residual flag leaf N concentration under O_3 exposure, despite not finding a difference in senescence onset, suggesting that the accelerated senescence and subsequent reduced N remobilisation efficiency is not the only factor increasing the residual N concentration in plant parts. Some researchers have suggested the increase occurs as defence proteins accumulate (Brewster, Fenner and Hayes, 2024; Sarkar et al., 2010). In the present study, we simulate the accelerated senescence that occurs under O_3 exposure, and we model the reduced remobilisation using simple linear equations (Eq. (2) and (3)). Future work to understand the mechanism for the increase in residual N in the stem and leaf would help refine the model to more accurately plant processes.

Brewster, Fenner and Hayes (2024) found that N fertilisation reduced the N left in the leaf and stem at harvest under O_3 exposure, delaying senescence and protecting chlorophyll against O_3 damage. The current model construct does not simulate this effect and assumes the plant receives optimum N. No N stress or extra fertilisation was considered. Future iterations of this model incorporating soil N processes could use the work of Brewster, Fenner and Hayes (2024) to include N fertilisation and model the ameliorative effect of variable N fertilisation on O_3 damage. Additionally, this first iteration of the model does not include any feedback of plant N status on photosynthetic or growth processes. Future research may want to consider the feedbacks between leaf N levels and photosynthetic rate, with higher leaf N increasing photosynthetic rate, which could offset O_3 induced reductions (Pilbeam, 2010). Researchers may also want to consider the influence of a higher leaf N in potentially delaying O_3 induced early senescence onset (Nehe et al., 2020; Martre et al., 2006).

5.5 Sensitivity analysis results

The sensitivity analysis (Fig.'s 9a and 9b) showed that the effect of varying leaf and stem remobilisation contributed little, if at all, to variations in grain N content or grain N% under the differing O_3 treatments. Further, the most influential parameter on grain N content and grain N%, was senescence onset; this does not change regardless of the O_3 treatment simulated. These results align with existing literature, which show that a shorter duration for grain fill leads to less time for nutrient remobilisation, subsequently impacting grain quality (Havé et al., 2017). Therefore, it is expected that the senescence parameters would have a large influence on grain N. Further, since the onset of leaf senescence is the beginning of leaf N remobilisation to the grain, it has a larger influence on grain N content and concentration than the end of leaf senescence (Havé et al., 2017). Therefore, for the Skyfall cultivar, under the O_3 conditions simulated, senescence onset has greater influence on grain quality than O_3 interruptions to remobilisation from an unspecified process. In our sensitivity analysis we observed a difference in the magnitude of S1 (the uncertainty in the output variable that is attributed to varying only that parameter) and ST (the uncertainty in the output variable that is attributed to varying a chosen parameter in combination with the other selected parameters) (Saltelli et al., 2008) between the different O_3 treatments. The non-linear response is unsurprising given the complex and interconnected nature of crop modelling. However, it isn't possible to determine whether this response is typical for wheat, since the present study considers data for only one cultivar and one location. If future work investigates multiple growing locations and wheat varieties and uncovers a similar response of the sensitivity indices for the differing O_3 concentrations, then the underlying crop modelling processes could be investigated to determine the reason for this effect.

5.6 Implications of sensitivity analysis results for growers

The sensitivity analysis results pose interesting questions around the importance of cultivars having an earlier or delayed senescence for maximising grain protein under O_3 exposure. Generally, a delayed onset of leaf senescence decreases grain protein content as there is a delay to the start of N remobilisation from the leaves to the grain (Havé et al., 2017; Sultana et al., 2021). A delayed senescence also decreases grain protein%, due to the reduction in grain N content and an increased length of photosynthetic activity that increases grain yield (Sultana et al., 2021; Nehe et al., 2020; Bogard et al., 2011). However, this is not always the case as there are several interacting effects from the environment (e.g. temperature, drought, O_3 or pathogens), N application and gene expression (Zhao et al., 2015; Nehe et al., 2020; Bogard et al., 2011; Gaju et al., 2014; Sultana et al., 2021). Stay-green cultivars have previously been identified as allowing plants to maintain their photosynthetic capacity under heat and drought stress conditions (Kamal et al., 2019). Since O_3 damage is ROS mediated, similar to the damage from heat and drought stress (Khanna-Chopra, 2012), it is expected that stay-green cultivars will provide a similar increased yield for O_3 exposed wheat by delaying the stress induced early senescence onset. The impact of using stay-green cultivars on wheat grain protein under O_3 stress conditions is yet to be investigated. However, a decrease in grain protein content under O_3 exposure may be due to the delayed onset of remobilisation (Havé et al., 2017; Sultana et al., 2021). Zhao et al. (2015) genetically modified wheat plants to investigate the response of senescence, grain yield and grain N% when a senescence delaying gene was over-expressed. In the genetically modified wheat, the grain yields were similar to the control, but grain N% was increased (Zhao et al., 2015). Therefore, stay green wheat cultivars that do not experience a grain protein penalty should be considered by breeders and investigated for their suitability under differing O_3 concentrations.

5.7 Potential model applications

Simulations of crop N content can be easily converted into protein through the use of a simple conversion factor, or linear regressions if N or water stress conditions are present that have not been accounted for previously in the simulation (Mariotti, Tomé and Mirand, 2008; Liu et al., 2018; Tkachuk, 1969). Therefore, grain protein% can easily be obtained from grain N%. Further, by using protein%, amino acid concentrations can be simulated using regressions developed by Liu et al. (2019), allowing the model to be extended to simulate protein quality. In addition, by building on the work of Broberg et al. (2015) it would also be possible to link changes in N content under O_3 exposure, to changes in other grain mineral contents, such as zinc, magnesium and starch. Such relations would be simple to integrate given the model already simulates O_3 effects on N, and there seem to be similarities between the effect of O_3 on N and the effect of O_3 on other minerals (Broberg et al., 2015). These improvements would increase the nutritional relevance of the model.

The DO_3SE-Crop model takes inputs of temperature, PPFD, CO_2 concentrations and precipitation. There is also a built in soil moisture module which can simulate the effect of water stress on stomatal O_3 flux (Büker et al., 2012). Because of these features, the DO_3SE model is an ideal candidate for simulating the combined effects of O_3 pollution and climate change on

crop yields. With the newly developed N module, this would allow the user to determine how O_3 pollution and climate change effects may interact to affect crop yield, quantity and quality, and hence dietary nutrition.

6. Conclusions

625   In summary, this study identified the key mechanisms for modelling N in wheat as soil N uptake, partitioning of N taken up from the soil between the leaf and stem, remobilisation of N from the leaves and stem to the grain, and the impact of O_3 on N remobilisation. Using these key processes, a new model was developed that can be used in combination with the existing O_3 deposition crop model, DO_3SE-Crop, to simulate the O_3 impact on wheat N. The newly developed model is the first to simulate the effect of O_3 on N in any plant species. After evaluation, a sensitivity analysis was applied to the model to identify the key

630   plant process that affects grain quality under O_3 exposure. It was found that O_3 induced early senescence onset was the key plant processes affecting grain quality under O_3 exposure, regardless of O_3 treatment. We recommend that breeders focussing on stay-green cultivars aim to develop cultivars that do not suffer a protein penalty. If such cultivars can maintain their yield and quality under abiotic stresses, they may also be tolerant to O_3 in terms of both yield and crop quality; testing this would be beneficial to further understand the implications of O_3 on global food and nutritional security.

Appendix A. DO₃SE-CropN

635   Detailed below are the equations and references for the N module of the DO_3SE-Crop N module. We found Wang & Engel's (2002) approach to writing up their crop model to be very effective so we take inspiration from their approach and present a description of the processes and references in the text, and tabulate the specific equations, with their corresponding references in each section. The values of parameters used in the module and their corresponding sources are tabulated also. For a full

640   mathematical description of the phenology, photosynthesis, carbon allocation and ozone damage processes of DO_3SE-Crop, please refer to Pande et al. (2024).

At the current stage of development, the N module is not integrated within DO_3SE-Crop. It requires the output file from a DO_3SE-Crop run in order to perform the N simulations.

A.1 N Uptake

645   Pre-anthesis a maximum N uptake ($NUP_{pre,max}, in\ gN\ m^{-2}\ day^{-1}$) is defined (Soltani and Sinclair, 2012). The actual N uptake by the crop pre-anthesis ($NUP_{pre}, gN\ m^{-2}\ day^{-1}$) is calculated using the work of Soltani and Sinclair (2012). Daily N uptake is the sum of the N associated with the increase in LAI that day ($LAI_{growth}, m^2\ day^{-1}$), the increase in dry matter of the stem that day ($DW_{stem\_grth}, g\ DW\ m^{-2}\ day^{-1}$) and the N deficit that day ($N_{stem,deficit}, g\ N\ m^{-2}\ day^{-1}$), that has been accumulated over the plant's life:

$$NUP_{pre} = DW_{stem\_grth} \times [N_{stem,target}] + LAI_{growth} \times [N_{leaf,target}] + N_{stem,deficit}. \tag{A1}$$

$[N_{stem,target}]$ is the target N concentration of the stem and $[N_{leaf,target}]$ is the target N concentration of the leaf (Soltani and Sinclair, 2012). The $N_{stem,deficit}$ is defined as the difference between the target stem N for its mass, and its current N content (N_{stem}):

$$N_{stem,deficit} = DW_{stem} \times [N_{stem,target}] - N_{stem}. \tag{A2}$$

where DW_{stem} is the dry weight of the stem in $g\ m^{-2}$. If $NUP_{pre} > NUP_{pre,max}$ we set $NUP_{pre} = NUP_{pre,max}$, otherwise, the crop takes up N equal to NUP_{pre}.

Post-anthesis, N uptake is a function associated with the capacity of the stem to hold nitrogen. The basis for this equation is taken from SiriusQuality (Martre et al., 2006). The potential N uptake post anthesis ($NUP_{post,pot}\ gN\ m^{-2}\ day^{-1}$), is calculated as follows:

$$NUP_{post,pot} = NUP_{post,max} \times \frac{T_{grainfill} - T}{T_{grainfill}} \tag{A3}$$

where $NUP_{post,max}$ is the maximum N uptake post-anthesis, $T_{grainfill}$ is the thermal time (in °C days) between the end of grain filling (i.e. harvest in the present model) and the start of anthesis, and T is the current thermal time (in °C days) since anthesis. Subsequently, the stems target capacity to hold N is calculated and compared to the current amount of N stored in the stem. If the current stem N, N_{stem} in $g\ N\ m^{-2}$, exceeds the target capacity, no N is taken up that day (equation (A4)).

$$NUP_{post} = 0\ if\ \ N_{stem} \geq DW_{stem} \times [N_{stem,target}] \tag{A4}$$

If the current stem N is less than the target capacity, the N taken up is equal to the minimum of the stem's current capacity and the potential uptake.

$$NUP_{post} = min(NUP_{post,pot}, DW_{stem} \times [N_{stem,target}] - N_{stem}) \tag{A5}$$

Table A1: Citations and names for equations describing soil N uptake

Equation number	Equation name	Developed according to…
(A1)	Actual plant N uptake pre-anthesis	(Soltani & Sinclair, 2012)
(A2)	N stem deficit	(Soltani & Sinclair, 2012)
(A3)	Potential daily N uptake post-anthesis	(Martre et al., 2006)
(A4)	Post-anthesis N uptake if current stem N is greater than target	developed in this study to ensure stem does not get an unlimited supply of N

| | (A5) | Post-anthesis N uptake if current stem N is less than target | (Martre et al., 2006) and adapted in this study to account for current stem N |

665

Table A2: Default and present parameterisations for the N module along with citations as to where the original default value was obtained

Parameter	Original Value	Value used in this study	Source for original value
$NUP_{post,max}$	$0.4\ g\ N\ m^{-2}\ day^{-1}$	$0.4\ g\ N\ m^{-2}\ day^{-1}$	(Martre et al., 2006)
$NUP_{pre,max}$	$0.25\ g\ N\ m^{-2}\ day^{-1}$	$0.65\ g\ N\ m^{-2}\ day^{-1}$	(Soltani and Sinclair, 2012)
$[N_{stem,target}]$	$0.015\ g\ N\ g^{-1}\ DW$	$0.018\ g\ N\ g^{-1}\ DW$	(Soltani and Sinclair, 2012)
$[N_{leaf,target}]$	$1.5\ g\ N\ m^{-2}$	$1.65\ g\ N\ m^{-2}$	(Soltani and Sinclair, 2012)

A.2 N partitioning to the stem and leaf

670 Pre-anthesis, the equations describing how the uptake of N is split between the leaf and stem are based on the work of Soltani and Sinclair (2012), and no N is allocated to the grains at this time. The stem and leaf have a defined target and minimum N concentration which can be calibrated for different wheat cultivars. In Soltani and Sinclair (2012) both the target and minimum stem and leaf N concentrations are constants. In this study, the minimum N concentrations of the leaf and stem are variable based on the ozone concentrations. This allows a reduction in remobilisation of N from the leaf and stem to the grain, as found

675 by Brewster et al. (2024), under higher ozone concentrations. It is easiest to see the structure of the N partitioning code in Fig. A1. The write up of pre-anthesis N partitioning to the leaves and stem is split into 2 sections based on whether the stem is experiencing a N deficit (i.e. stem N is less than its minimum).
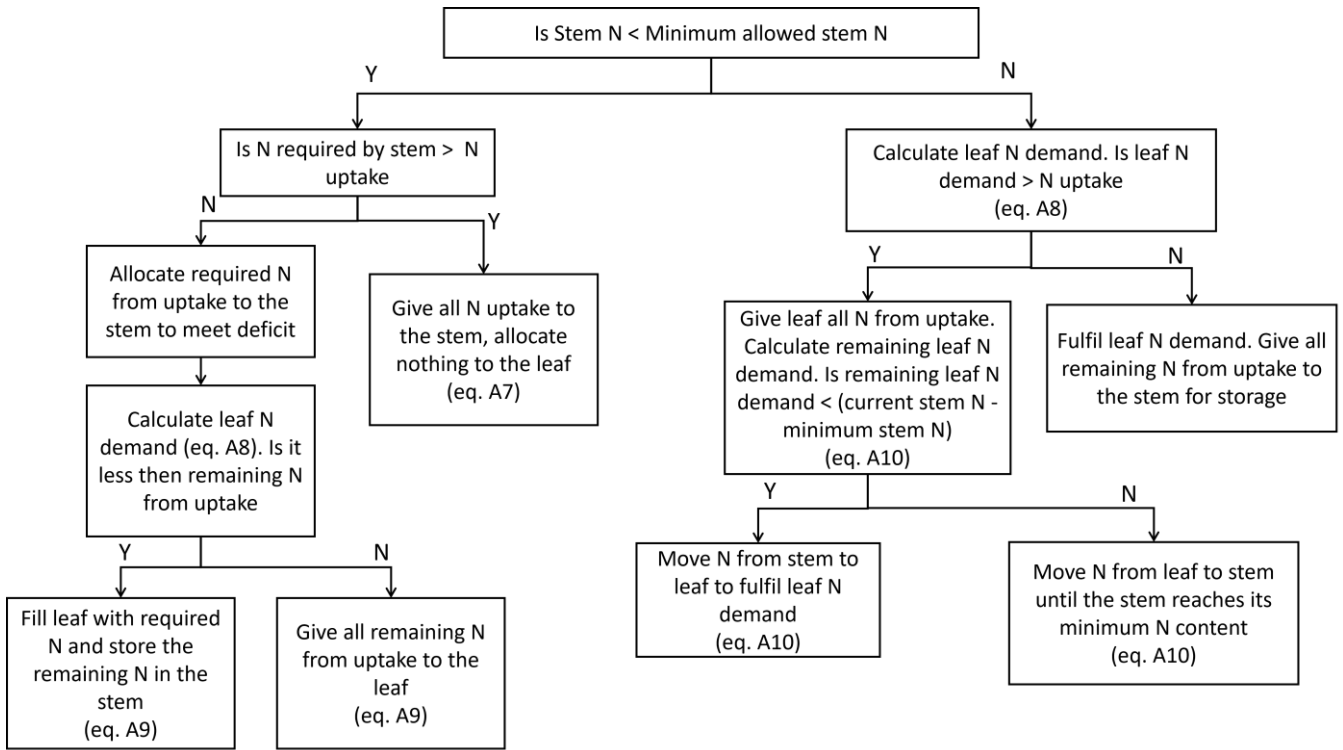
Fig. A1: Figure showing the allocation of N to the stem and leaf before anthesis. Y and N represent "yes" and "no" respectively.
Equation definitions are referenced appropriately. Where equation numbers are not indicated additional information can be found
in the text. Equations and model structure for N allocation are based on those of Soltani & Sinclair (2012) and modified for the
purposes of this study.

Firstly, the current stem N concentration is compared to the minimum allowed stem N concentration, $\left[N_{stem,min}\right]$.

A.2.1 If Current stem N concentration is less than the minimum stem N concentration (N deficit)

If the current stem N concentration is less than the minimum concentration, then allocation of N to the stem is prioritised.

$$N_{req,stem} = DW_{stem} \times \left[N_{stem,min}\right] - N_{stem} \tag{A6}$$

where $N_{req,stem}$ is the N required by the stem to meet its deficit in $g\,N\,m^{-2}$. If $N_{req,stem}$ is greater than the amount of N taken

up that day ($NUP, g\,N\,m^{-2}$), the N entering the stem pool ($N_{into,stem}, g\,N\,m^{-2}$) is capped at the amount of N taken up.

$$if\ N_{req,stem} > NUP_{pre} \begin{cases} N_{into,stem} = NUP \\ N_{leaving,leaf} = 0 \\ N_{leaving,stem} = 0 \\ N_{into,leaf} = 0 \end{cases} \tag{A7}$$

Equation (A7) has been modified from Soltani & Sinclair (2012) who allow leaf area to senesce and provide the stem with N

if there is not enough to meet the stem's N demand. The senescing of leaf area to provide N was removed in the current iteration

31

of DO$_3$SE-CropN. Currently, there is no interdependencies between the N module and DO$_3$SE-Crop. The DO$_3$SE-Crop model runs and then the N module is applied to the output of DO$_3$SE-Crop to calculate crop N. It is therefore not possible to senesce leaf area to provide N in the current version of the N module as the leaf area was already determined in DO$_3$SE-Crop.

695 If there was enough N to meet the deficit of the stem, then $N_{into,stem} = N_{req,stem}$ and $N_{leaving,stem} = 0$. Then, the N required for maintaining leaf area growth at its target N concentration ($N_{req,leaf}$, $g\ N\ m^{-2}$) is calculated using equation (A8).

$$N_{req,leaf} = LAI_{growth} \times [N_{leaf,target}] \tag{A8}$$

If $N_{req,leaf}$ can be fulfilled by the N left over after maintaining the stem growth at minimum N concentration, then N is partitioned to the leaves and any leftover N is partitioned to the stem for storage. If the leftover N cannot fulfil the demand of the leaf, then the remaining N from uptake is partitioned to the leaves (Soltani and Sinclair, 2012).

$$N_{into,leaf} = \begin{cases} N_{req,leaf} & if\ N_{req,leaf} \leq NUP - N_{into,stem} \\ NUP - N_{into,stem} & if\ N_{req,leaf} > NUP - N_{into,stem} \end{cases} \tag{A9}$$

700 **A.2.2 If Current stem N concentration is not less than the minimum stem N concentration (no N deficit)**

If the stem N is not below its minimum, then N is first allocated to the leaves. The N required by the leaves is calculated in accordance with equation (A8). If the N required by the leaves is less than the N uptake that day, the N required by the leaves is transferred to them: $N_{into,leaf} = N_{req,leaf}$ and $N_{leaving,leaf} = 0$. Subsequently, the remaining N from uptake is transferred to the stem, $N_{into,stem} = NUP - N_{into,leaf}$ and $N_{leaving,stem} = 0$

705 If the leaves required more N than was taken up by the crop, the extra demand is fulfilled by using some of the stem N. The N from the stem is removed only until the stem reaches its minimum concentration.

$$N_{leaving,stem} = \begin{cases} 0 & if\ N_{req,leaf} \leq NUP \\ \min\ (N_{req,leaf} - NUP,\ N_{stem} - (DW_{stem} \times [N_{stem,min}]) & if\ N_{req,leaf} > NUP \end{cases} \tag{A10}$$

In equation (A10), the minimum function ensures that the stem N does not fall below its minimum. In the scenario that the leaves required more N than taken up by the crop, $N_{leaving,leaf} = 0$ and $N_{into,stem} = 0$.

710

Table A3: Citations and names for equations describing N partitioning to the stem and leaf

Equation number	Equation name	Developed according to…
(A6)	The N required by the stem for growth	(Soltani and Sinclair, 2012)

(A7)	The N partitioned to the leaf and stem if the stem has a N deficiency and N uptake is not great enough to meet it	(Soltani and Sinclair, 2012) and adapted to remove leaf senescence releasing N in this study
(A8)	The N required for leaf area expansion	(Soltani and Sinclair, 2012)
(A9)	The N going into the leaf pool if N uptake met the stem N deficit	(Soltani and Sinclair, 2012)
(A10)	The N leaving the stem to maintain leaf area expansion under no stem N deficit	(Soltani and Sinclair, 2012) and adapted in this study to ensure stem N does not go below its minimum

A.3 N partitioning to the grain
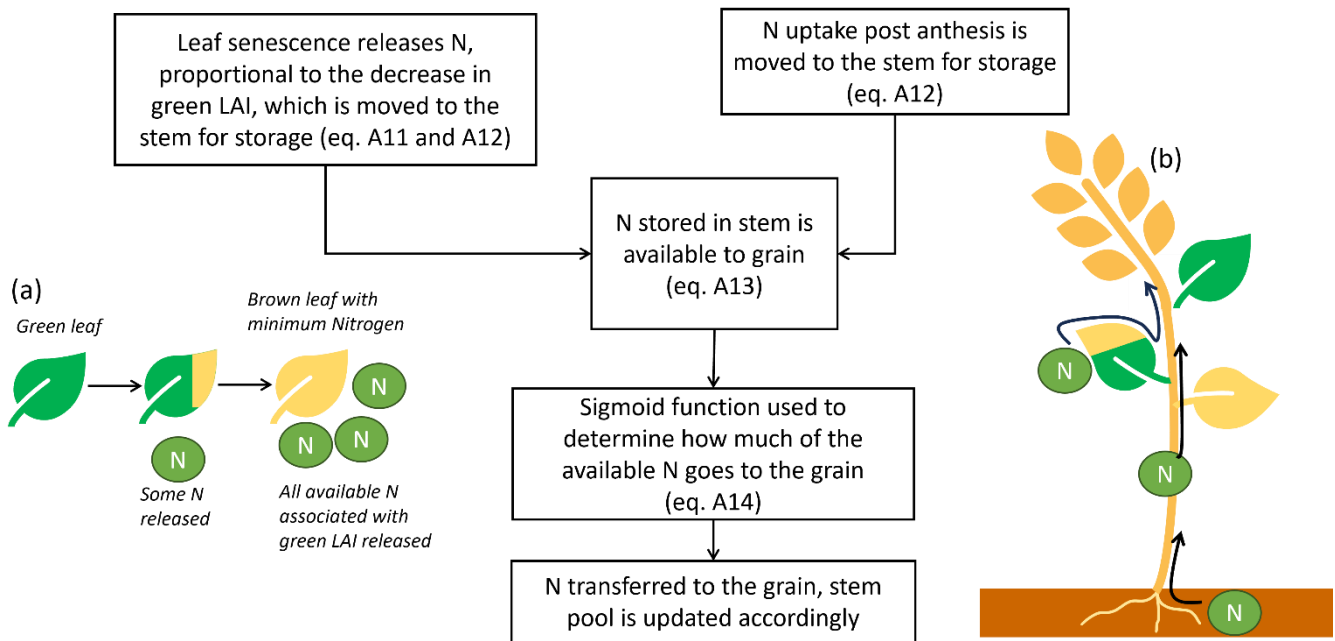
Fig. A2: Figure showing the allocation of N to the wheat grains post-anthesis with equations indicated appropriately. Sub-image (a) is a visual representation of a leaf releasing N as the leaf area senesces. Sub-image (b) shows the 3 locations where N is transferred to the grain from: post anthesis N uptake, N stored in the stem, senescing leaf area.

After anthesis, the grain begins to fill with N and the model equations change to reflect that the priority is grain fill, not leaf area expansion or growth. After anthesis $N_{into,leaf} = 0$ always. As leaf area senesces, N is released:

$$N_{leaving,leaf} = \left(LAI_{yesterday} - LAI_{today} \right) \times \left(\frac{N_{leaf}}{LAI_{yesterday}} - \left[N_{leaf,min} \right] \right) \tag{A11}$$

where $LAI_{yesterday}$ and LAI_{today} represent the values of the leaf area index yesterday and today as calculated in DO$_3$SE-Crop. N released from the leaf, and N taken up by the plant post-anthesis are added to the stem N pool for storage, as they would have to travel through the stem to reach the grains (Sanchez-Bragado, Serret and Araus, 2017). The stem Nitrogen is then updated accordingly:

$$N_{into,stem} = N_{leaving,leaf} + NUP_{post} \qquad (A12)$$

Not all of the N in the stem is available to be transferred to the grain as the stem has a minimum N concentration. Therefore, the available stem N (often referred to as the labile pool in other crop models) is calculated as:

$$N_{available} = N_{stem} - \left(DW_{stem} \times [N_{stem,min}]\right) \qquad (A13)$$

The fraction of $N_{available}$ that is transferred to the grain each day is determined through a sigmoid function. The sigmoid was chosen as it uses only two extra parameters which allows the start and rate of grain fill with N to be customised without the addition of much complexity. The N in the $N_{available}$ pool can be transferred to the grain, or it can remain as part of the stem. The sigmoid determines the fraction of N going to the grain from $N_{available}$. The fraction increases as the plant develops. Multiplying $N_{available}$ by the sigmoid function gives the amount of N transferred to the grain that day. α_N and β_N are the coefficients that customise the onset and rate of grain fill. They can be calibrated to customise grain fill.

$$N_{to\_grain} = N_{available} \times \frac{1}{1 + exp(-\alpha_N(dvi - \beta_N))} \qquad (A14)$$

Once N has been transferred to the grain, the leaf and stem N pools are decreased according to their N availability to account for this transfer. Fig. A2 diagrammatically represents the grain filling process and Fig. A3 shows an illustration of the sigmoid function with varying parameterisations to control grain fill.
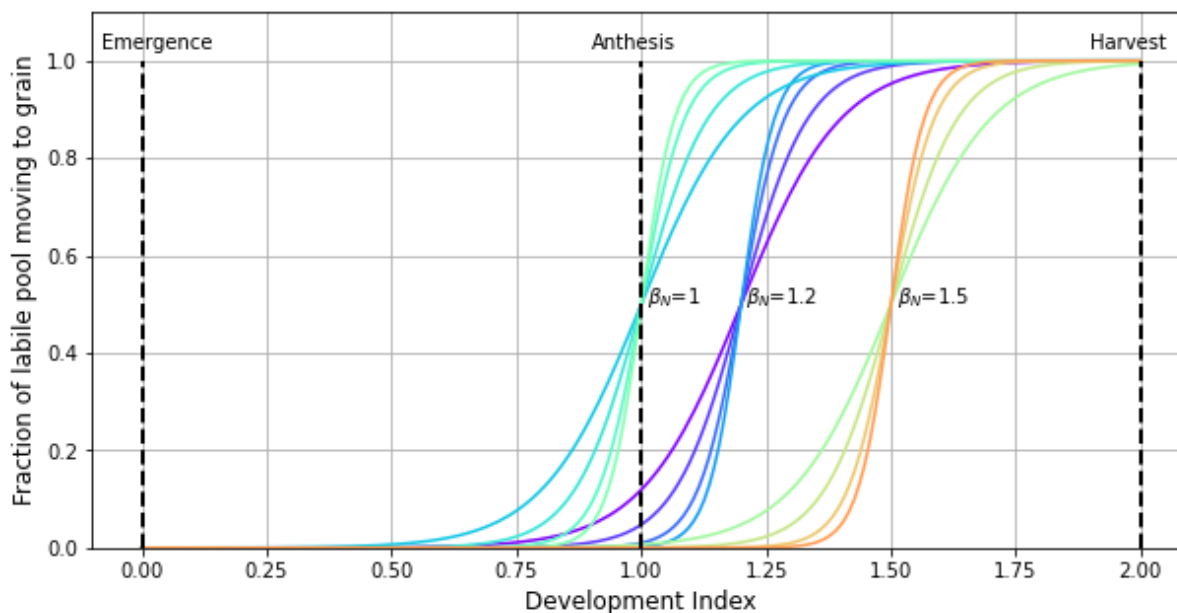
735

Fig. A3: Plot showing example parameterisations of α_N and β_N for customising the sigmoid function describing the fraction of labile N moving to the grain. For each value of β_N, values of α_N of 10, 15, 23 and 30 are plotted to show how the rate, start and end of grain fill can be customised. Though $\beta_N = 1$ has been plotted to illustrate how the shape of the function can be customised, care should be taken if using this value, as for lower values of α_N it can imply grain filling with N begins midway between emergence
740 **and anthesis. Sensible parameterisations should be chosen.**

Table A4: Citations and names for equations describing grain filling with N

Equation number	Equation name	Developed according to…
(A11)	N released from senescing leaves	Based on the equations in Soltani & Sinclair (2012)(Soltani and Sinclair, 2012) describing release of N from the leaves, but adapted for this study to match desired variables
(A12)	Update stem N pools	(this study)
(A13)	Calculate available N in stem	Based on the equations in Soltani & Sinclair (2012)(Soltani and Sinclair, 2012) describing release of N from the stem, but adapted for this study to match desired variables and incorporate post anthesis N uptake
(A14)	Grain N sigmoid function	(this study)

35

Table A5: Parameterisation of alpha and beta parameters for grain filling

Parameter	Value used in this study	Source
α_N	23	(this study)
β_N	1.2	(this study)

A.4 Ozone impact on N remobilisation

The effect of ozone on grain N has been described in the main body of this study but will be discussed with relation to the equations and how they link with the previously described model structure here. Broberg et al. (2017) and Brewster et al. (2024) found that as ozone concentrations increased, the fraction of N in the leaf and stem at harvest, that was present at anthesis, increased. In essence, the remobilisation of N from the leaves and stem to the grains decreased. A regression of the combined data from Broberg et al. (2017) and Brewster et al. (2024) representing the remobilisation is shown in Fig. 2 of the main body of the study.

To represent the reduced remobilisation under increased ozone exposure, the remobilisation regression was used to calculate new values of $[N_{stem,min}]$ and $[N_{leaf,min}]$ under ozone exposure. The fraction of N remaining in the leaf and stem at harvest that was there at anthesis (fN_{remob}) is approximated by:

$$fN_{remob} = \frac{DM_{leaf,harv} \times [N_{leaf,min}] + DM_{stem,harv} \times [N_{stem,min}]}{DM_{leaf,anth} \times [N_{leaf,targ}] + DM_{stem,anth} \times [N_{stem,targ}]} \tag{A15}$$

Equation (A15) assumes the anthesis leaf and stem N concentration is the same as the target N concentration, as the first iteration of the model assumes no N limitation. Additionally, for calibration purposes, the "harvest" N concentration was assumed to be the same as the minimum N concentration. In the model itself this would not occur as not all available N will be remobilised due to ozone effects on senescence. However, for calibration purposes equation (A15) is a good approximation. Using equation (A15), minimum values of leaf and stem N for the differing ozone treatments were manually altered for each ozone concentration, to estimate values for the N remobilisation (red points on Fig. 2) that form a linear regression fitting inside the 95% CI. The leaf and stem minimum N concentrations of each red point were extracted. The minimum leaf N concentration, and minimum stem N concentration, were regressed separately with M12 to give regressions describing how the minimum N concentration in the plant part varies with ozone concentration:

$$\frac{[N_{leaf,min}]}{1\ gN\ LAI^{-1}} \times 100 = m_{leaf} \times \frac{[O_{3,M12}]}{1\ ppb} + c_{leaf} \tag{A16}$$

$$\frac{[N_{stem,min}]}{1\ gN\ DM^{-1}} \times 100 = m_{leaf} \times \frac{[O_{3,M12}]}{1\ ppb} + c_{stem} \tag{A17}$$

Table A6: Citations and names for equations describing the O₃ effect on N remobilisation

Equation number	Equation name	Developed according to…
(A15)	The fraction of N remaining in the leaf and stem at harvest that was there at anthesis	(this study)
(A16)	Ozone effect on minimum leaf N concentration	(this study)
(A17)	Ozone effect on minimum stem N concentration	(this study)

Table A7: Parameterisation of parameters associated with the ozone effect on N grain filling as used in the DO₃SE-CropN model

Parameter	Value	Source
m_{leaf}	0.798	(this study)
m_{stem}	0.0138	(this study)
c_{leaf}	10.89	(this study)
c_{stem}	0.2293	(this study)

A.5 Ozone impact on N remobilisation

In the DO₃SE-Crop model, green leaves are photosynthesising leaves, and brown leaves are senesced leaves. In the N module, the N associated with the senesced LAI is released (as described in section 1.3). Leaf area which has senesced will have the minimum leaf N concentration. Green leaf area which has not senesced will have a higher N concentration. An average leaf N concentration can be calculated by taking the absolute N in both green and brown leaves and dividing it by the total (green + brown) leaf DM.

Code availability

An open version of the DO₃SE-Crop model, version 4.39.11 as used in the present study can be found at Bland (2024) and version 1.0 of the N module for DO₃SE-Crop is found at Cook (2024).

Data availability

Author contributions

Funding

Competing interests

The authors declare that they have no conflict of interest.

References

Agathokleous, E., Kitao, M. and Calabrese, E. J. (2019). Hormesis: A Compelling Platform for Sophisticated Plant Science. *Trends in Plant Science*, 24 (4), pp.318–327. [Online]. Available at: doi:10.1016/j.tplants.2019.01.004.

Baqasi, L. A. et al. (2018). Effects of low concentrations of ozone (O3) on metabolic and physiological attributes in wheat (Triticum aestivum L.) pants. *Biomedical and Pharmacology Journal*, 11 (2), pp.929–934. [Online]. Available at: doi:10.13005/bpj/1450.

805   Barraclough, P. B., Lopez-Bellido, R. and Hawkesford, M. J. (2014). Genotypic variation in the uptake, partitioning and remobilisation of nitrogen during grain-filling in wheat. *Field Crops Research*, 156, pp.242–248. [Online]. Available at: doi:10.1016/j.fcr.2013.10.004.

Bertheloot, J. et al. (2008). A process-based model to simulate nitrogen distribution in wheat (Triticum aestivum) during grain-filling. *Functional Plant Biology*, 35 (10), pp.781–796. [Online]. Available at: doi:10.1071/FP08064.

810   Bielenberg, D. G., Lynch, J. P. and Pell, E. J. (2002). Nitrogen dynamics during O3-induced accelerated senescence in hybrid poplar. *Plant, Cell and Environment*, 25 (4), pp.501–512. [Online]. Available at: doi:10.1046/j.1365-3040.2002.00828.x.

Bland, S. (2024). *SEI-DO3SE/pyDO3SE-open: V4.39.11 (v4.39.11)*. Zenodo. [Online]. Available at: doi:10.5281/zenodo.11620482.

Bogard, M. et al. (2011). Anthesis date mainly explained correlations between post-anthesis leaf senescence, grain yield, and
815   grain protein concentration in a winter wheat population segregating for flowering time QTLs. *Journal of Experimental Botany*, 62 (10), pp.3621–3636. [Online]. Available at: doi:10.1093/jxb/err061.

Brewster, C. (2023). *Ground level ozone and wheat: an exploration of effects on yield, interactions with nitrogen, and potential sources of sensitivity and tolerance*. [Online]. Available at: https://research.bangor.ac.uk/portal/en/theses/ground-level-ozone-and-wheat-an-exploration-of-effects-on-yield-interactions-with-nitrogen-and-potential-sources-of-sensitivity-and-
820   tolerance(88cc93b5-e504-4006-a0a9-69613e730e8c).html.

Brewster, C., Fenner, N. and Hayes, F. (2024). Chronic ozone exposure affects nitrogen remobilization in wheat at key growth stages. *Science of the Total Environment*, 908 (168288). [Online]. Available at: doi:10.1016/j.scitotenv.2023.168288.

Broberg, M. C. et al. (2015). Ozone effects on wheat grain quality - A summary. *Environmental Pollution*, 197, pp.203–213. [Online]. Available at: doi:10.1016/j.envpol.2014.12.009.

825   Broberg, M. C. et al. (2017). Fertilizer efficiency in wheat is reduced by ozone pollution. *Science of the Total Environment*, 607–608, pp.876–880. [Online]. Available at: doi:10.1016/j.scitotenv.2017.07.069.

Broberg, M. C. et al. (2019). Effects of elevated CO2 on wheat yield: Non-linear response and relation to site productivity. *Agronomy*, 9 (5), pp.1–18. [Online]. Available at: doi:10.3390/agronomy9050243.

Broberg, M. C. et al. (2021). Harvest index and remobilization of 13 elements during wheat grain filling: Experiences from
830   ozone experiments in China and Sweden. *Field Crops Research*, 271 (July). [Online]. Available at: doi:10.1016/j.fcr.2021.108259.

Broberg, M. C. et al. (2023). Effects of ozone, drought and heat stress on wheat yield and grain quality. *Agriculture, Ecosystems and Environment*, 352 (December 2022). [Online]. Available at: doi:10.1016/j.agee.2023.108505.

Büker, P. et al. (2012). DO3SE modelling of soil moisture to determine ozone flux to forest trees. *Atmospheric Chemistry and*
835   *Physics*, 12 (12), pp.5537–5562. [Online]. Available at: doi:10.5194/acp-12-5537-2012.

Cariboni, J. et al. (2007). The role of sensitivity analysis in ecological modelling. *Ecological Modelling*, 203 (1–2), pp.167–182. [Online]. Available at: doi:10.1016/j.ecolmodel.2005.10.045.

Chang-Espino, M. et al. (2021). The effect of increased ozone levels on the stable carbon and nitrogen isotopic signature of wheat cultivars and landraces. *Atmosphere*, 12 (7), pp.1–25. [Online]. Available at: doi:10.3390/atmos12070883.

840 Chenu, K. et al. (2017). Contribution of Crop Models to Adaptation in Wheat. *Trends in Plant Science*, 22 (6), pp.472–490. [Online]. Available at: doi:10.1016/j.tplants.2017.02.003.

Cho, K. et al. (2011). *Tropospheric ozone and plants: Absorption, responses, and consequences*. [Online]. Available at: doi:10.1007/978-1-4419-8453-1_3.

Cook, J. (2024). *JoCook1997/DO3SE-CropN: Initial release (v2.0)*. Zenodo. [Online]. Available at:
845 doi:10.5281/zenodo.13771475.

Dai, L. et al. (2019). Nitrogen availability does not affect ozone flux-effect relationships for biomass in birch (Betula pendula) saplings. *Science of the Total Environment*, 660, pp.1038–1046. [Online]. Available at: doi:10.1016/j.scitotenv.2019.01.092.

Emberson, L. et al. (2021). *Methodology for gap-filling and standardisation of data for AgMIP Ozone V8*. [Online]. Available at: https://agmipdatahub.files.wordpress.com/2021/10/agmip-gap-filling-protocol_-v8.docx.pdf [Accessed 17 April 2024].

850 Emberson, L. D. et al. (2009). A comparison of North American and Asian exposure-response data for ozone effects on crop yields. *Atmospheric Environment*, 43 (12), pp.1945–1953. [Online]. Available at: doi:10.1016/j.atmosenv.2009.01.005.

Emberson, L. D. et al. (2018). Ozone effects on crops and consideration in crop models. *European Journal of Agronomy*, 100 (June), pp.19–34. [Online]. Available at: doi:10.1016/j.eja.2018.06.002.

Ewert, F. and Porter, J. R. (2000). Ozone effects on wheat in relation to CO2: Modelling short-term and long-term responses
855 of leaf photosynthesis and leaf duration. *Global Change Biology*, 6 (7), pp.735–750. [Online]. Available at: doi:10.1046/j.1365-2486.2000.00351.x.

FAO. (2017). *The future of food and agriculture: trends and challenges*. Rome. [Online]. Available at: https://www.fao.org/policy-support/tools-and-publications/resources-details/en/c/472484/.

FAO et al. (2020). *The State of Food Security and Nutrition in the World 2020. Transforming food systems for affordable*
860 *healthy diets.* Rome: FAO. [Online]. Available at: https://www.fao.org/policy-support/tools-and-publications/resources-details/en/c/1298217/.

Farquhar, G. D., Caemmerer, S. and Berry, J. A. (1980). A biochemical model of photosynthetic CO2 assimilation in leaves of C3 species. *Planta*, 149 (1), pp.78-90–90. [Online]. Available at: doi:10.1007/BF00386231.

Fatima, A. et al. (2018). Variability in defence mechanism operating in three wheat cultivars having different levels of
865 sensitivity against elevated ozone. *Environmental and Experimental Botany*, 155 (June), pp.66–78. [Online]. Available at: doi:10.1016/j.envexpbot.2018.06.015.

Fatima, A. et al. (2019). Ascorbic acid and thiols as potential biomarkers of ozone tolerance in tropical wheat cultivars. *Ecotoxicology and Environmental Safety*, 171 (January), pp.701–708. [Online]. Available at: doi:10.1016/j.ecoenv.2019.01.030.

870 Feller, U. and Fischer, A. (1994). Nitrogen metabolism in senescing leaves. *Critical Reviews in Plant Sciences*, 13 (3), pp.241–273. [Online]. Available at: doi:10.1080/07352689409701916.

40

Feng, Z., Kobayashi, K. and Ainsworth, E. A. (2008). Impact of elevated ozone concentration on growth, physiology, and yield of wheat (Triticum aestivum L.): A meta-analysis. *Global Change Biology*, 14 (11), pp.2696–2708. [Online]. Available at: doi:10.1111/j.1365-2486.2008.01673.x.

875 Fowler, D. et al. (2008). *Ground-level ozone in the 21st century: future trends, impacts and policy implications*. (October). [Online]. Available at: https://royalsociety.org/news-resources/publications/2008/ground-level-ozone/.

Fu, T. M. and Tian, H. (2019). Climate Change Penalty to Ozone Air Quality: Review of Current Understandings and Knowledge Gaps. *Current Pollution Reports*, 5 (3), pp.159–171. [Online]. Available at: doi:10.1007/s40726-019-00115-6.

Gaju, O. et al. (2014). Nitrogen partitioning and remobilization in relation to leaf senescence, grain yield and grain nitrogen

880 concentration in wheat cultivars. *Field Crops Research*, 155, pp.213–223. [Online]. Available at: doi:10.1016/j.fcr.2013.09.003.

Gelang, J. et al. (2000). Rate and duration of grain filling in relation to flag leaf senescence and grain yield in spring wheat (Triticum aestivum) exposed to different concentrations of ozone. *Physiologia Plantarum*, 110 (3), pp.366–375. [Online]. Available at: doi:10.1111/j.1399-3054.2000.1100311.x.

885 Guarin, J. R. et al. (2019). Modeling the effects of tropospheric ozone on wheat growth and yield. *European Journal of Agronomy*, 105 (February), pp.13–23. [Online]. Available at: doi:10.1016/j.eja.2019.02.004.

Guo, J. et al. (2021). Proteomics reveals the effects of drought stress on the kernel development and starch formation of waxy maize. *BMC Plant Biology*, 21 (1), pp.1–14. [Online]. Available at: doi:10.1186/s12870-021-03214-z.

Havé, M. et al. (2017). Nitrogen remobilization during leaf senescence: Lessons from Arabidopsis to crops. *Journal of*

890 *Experimental Botany*, 68 (10), pp.2513–2529. [Online]. Available at: doi:10.1093/jxb/erw365.

Herman, J. and Usher, W. (2019). *SALib Documentation*. [Online]. Available at: https://salib.readthedocs.io/_/downloads/en/latest/pdf/.

Kamal, N. M. et al. (2019). Stay-green trait: A prospective approach for yield potential, and drought and heat stress adaptation in globally important cereals. *International Journal of Molecular Sciences*, 20 (23). [Online]. Available at:

895 doi:10.3390/ijms20235837.

Kang, J. et al. (2023). Physiological mechanisms underlying reduced photosynthesis in wheat leaves grown in the field under conditions of nitrogen and water deficiency. *Crop Journal*, 11 (2), pp.638–650. [Online]. Available at: doi:10.1016/j.cj.2022.06.010.

van Keulen, H. and Seligman, N. H. (1987). *Simulation of water use, nitrogen nutrition and growth of a spring wheat crop*.

900 Wageningen: Pudoc. [Online]. Available at: doi:10.1017/S0021859600081582.

Khanna-Chopra, R. (2012). Leaf senescence and abiotic stresses share reactive oxygen species-mediated chloroplast degradation. *Protoplasma*, 249 (3), pp.469–481. [Online]. Available at: doi:10.1007/s00709-011-0308-z.

Liu, J. et al. (2018). The effects of nitrogen and water stresses on the nitrogen-to-protein conversion factor of winter wheat. *Agricultural Water Management*, 210 (February), pp.217–223. [Online]. Available at: doi:10.1016/j.agwat.2018.07.042.

905   Liu, J. et al. (2019). Modeling wheat nutritional quality with a modified CERES-wheat model. *European Journal of Agronomy*, 109 (September 2018), p.125901. [Online]. Available at: doi:10.1016/j.eja.2019.03.005.

Liu, Y. et al. (2020). Dynamic responses of accumulation and remobilization of water soluble carbohydrates in wheat stem to drought stress. *Plant Physiology and Biochemistry*, 155 (July), pp.262–270. [Online]. Available at: doi:10.1016/j.plaphy.2020.07.024.

910   Mariem, S. Ben et al. (2021). Climate Change, Crop Yields, and Grain Quality of C3 Cereals: A Meta-Analysis of [CO2], Temperature , and Drought Effects. *Plants*, 10 (6), pp.1–19. [Online]. Available at: doi:10.3390/plants10061052.

Mariotti, F., Tomé, D. and Mirand, P. P. (2008). Converting nitrogen into protein - Beyond 6.25 and Jones' factors. *Critical Reviews in Food Science and Nutrition*, 48 (2), pp.177–184. [Online]. Available at: doi:10.1080/10408390701279749.

Martre, P. et al. (2006). Modelling protein content and composition in relation to crop nitrogen dynamics for wheat. *European Journal of Agronomy*, 25 (2), pp.138–154. [Online]. Available at: doi:10.1016/j.eja.2006.04.007.

915

Mills, G. et al. (2011). New stomatal flux-based critical levels for ozone effects on vegetation. *Atmospheric Environment*, 45 (28), pp.5064–5068. [Online]. Available at: doi:10.1016/j.atmosenv.2011.06.009.

Mills, G. et al. (2018a). Closing the global ozone yield gap: Quantification and cobenefits for multistress tolerance. *Global Change Biology*, 24 (10), pp.4869–4893. [Online]. Available at: doi:10.1111/gcb.14381.

920   Mills, G. et al. (2018b). Ozone pollution will compromise efforts to increase global wheat production. *Global Change Biology*, 24 (8), pp.3560–3574. [Online]. Available at: doi:10.1111/gcb.14157.

Mills, G. et al. (2018c). Tropospheric Ozone Assessment Report: Present-day ozone distribution and trends relevant to human health. *Elementa: Science of the Anthropocene*, 6 (47). [Online]. Available at: doi:10.1525/elementa.302.

Mishra, A. K., Rai, R. and Agrawal, S. B. (2013). Individual and interactive effects of elevated carbon dioxide and ozone on

925   tropical wheat (Triticum aestivum L.) cultivars with special emphasis on ROS generation and activation of antioxidant defence system. *Indian Journal of Biochemistry and Biophysics*, 50 (2), pp.139–149. [Online]. Available at: https://pubmed.ncbi.nlm.nih.gov/23720888/.

Nagarajan, S. et al. (1999). Effect of Post-Anthesis Water Stress on Accumulation of Dry Matter, Carbon and Nitrogen and Their Partitioning in Wheat Varieties Differing in Drought Tolerance. *Journal of Agronomy & Crop Science*, 183, pp.129–

930   136. [Online]. Available at: doi:10.1046/j.1439-037x.1999.00326.x.

Nehe, A. S. et al. (2020). Nitrogen partitioning and remobilization in relation to leaf senescence, grain yield and protein concentration in Indian wheat cultivars. *Field Crops Research*, 251 (November 2019), p.107778. [Online]. Available at: doi:10.1016/j.fcr.2020.107778.

Nguyen, T. H. et al. (2024). Assessing the spatio-temporal tropospheric ozone and drought impacts on leaf growth and grain

935   yield of wheat across Europe through crop modeling and remote sensing data. *European Journal of Agronomy*, 153 (September 2023). [Online]. Available at: doi:10.1016/j.eja.2023.127052.

Osborne, S. et al. (2019). New insights into leaf physiological responses to ozone for use in crop modelling. *Plants*, 8 (4). [Online]. Available at: doi:10.3390/plants8040084.

Osborne, T. et al. (2015). JULES-crop: A parametrisation of crops in the Joint UK Land Environment Simulator. *Geoscientific Model Development*, 8 (4), pp.1139–1155. [Online]. Available at: doi:10.5194/gmd-8-1139-2015.

Pande, P. et al. (2024a). Developing the DO3SE-crop model for Xiaoji , China. *EGUsphere [preprint]*. [Online]. Available at: doi:10.5194/egusphere-2024-694.

Pande, P. et al. (2024b). Ozone dose-response relationships for wheat can be derived using photosynthetic-based stomatal conductance models. *Agricultural and Forest Meteorology*, 356 (August 2023), p.110150. [Online]. Available at: doi:10.1016/j.agrformet.2024.110150.

Panozzo, J. F. and Eagles, H. A. (1999). Rate and duration of grain filling and grain nitrogen accumulation of wheat cultivars grown in different environments. *Australian Journal of Agricultural Research*, 50 (6), pp.1007–1015. [Online]. Available at: doi:10.1071/AR98146.

Paoletti, E. and Grulke, N. E. (2010). Ozone exposure and stomatal sluggishness in different plant physiognomic classes. *Environmental Pollution*, 158 (8), pp.2664–2671. [Online]. Available at: doi:10.1016/j.envpol.2010.04.024.

Pedregosa, F. et al. (2011). Scikit-learn: Machine Learning in Python Fabian. *Journal of Machine Learning Research*, 12, pp.2825–2830. [Online]. Available at: doi:10.48550/arXiv.1201.0490.

Piikki, K. et al. (2008). The grain quality of spring wheat (Triticum aestivum L.) in relation to elevated ozone uptake and carbon dioxide exposure. *European Journal of Agronomy*, 28 (3), pp.245–254. [Online]. Available at: doi:10.1016/j.eja.2007.07.004.

Pilbeam, D. J. (2010). *The Utilization of Nitrogen by Plants: A Whole Plant Perspective*. [Online]. Available at: doi:10.1002/9781444328608.ch13.

Rai, R. and Agrawal, M. (2012). Impact of tropospheric ozone on crop plants. *Proceedings of the National Academy of Sciences India Section B - Biological Sciences*, 82 (2), pp.241–257. [Online]. Available at: doi:10.1007/s40011-012-0032-2.

Saltelli, A. et al. (2008). *Global Sensitivity Analysis: The Primer*. Chichester: John Wiley & Sons Ltd. [Online]. Available at: doi:10.1111/j.1751-5823.2008.00062_17.x.

Sanchez-Bragado, R., Serret, M. D. and Araus, J. L. (2017). The nitrogen contribution of different plant parts to wheat grains: Exploring genotype, water, and nitrogen effects. *Frontiers in Plant Science*, 7 (January), pp.1–14. [Online]. Available at: doi:10.3389/fpls.2016.01986.

Sarkar, A. et al. (2010). Investigating the impact of elevated levels of ozone on tropical wheat using integrated phenotypical, physiological, biochemical, and proteomics approaches. *Journal of Proteome Research*, 9 (9), pp.4565–4584. [Online]. Available at: doi:10.1021/pr1002824.

scikit-learn developers. (2023). *sklearn.metrics.r2_score; scikit-learn 1.3.2 documentation*. [Online]. Available at: https://scikit-learn.org/stable/modules/generated/sklearn.metrics.r2_score.html [Accessed 17 April 2024].

Shiferaw, B. et al. (2013). Crops that feed the world 10. Past successes and future challenges to the role played by wheat in global food security. *Food Security*, 5 (3), pp.291–317. [Online]. Available at: doi:10.1007/s12571-013-0263-y.

Silvestro, P. C. et al. (2017). Sensitivity analysis of the Aquacrop and SAFYE crop models for the assessment of water limited winter wheat yield in regional scale applications. *PLoS ONE*, 12 (11), pp.1–30. [Online]. Available at: doi:10.1371/journal.pone.0187485.

975 Soltani, A. and Sinclair, T. R. (2012). *Modeling physiology of crop development, growth and yield*. Soltani, A. and Sinclair, T. R. (Eds). CAB International. [Online]. Available at: doi:10.1079/9781845939700.0001.

Sultana, N. et al. (2021). Wheat leaf senescence and its regulatory gene network. *Crop Journal*, 9 (4), pp.703–717. [Online]. Available at: doi:10.1016/j.cj.2021.01.004.

Szopa, S. et al. (2021). Short-lived Climate Forcers. In: Masson-Delmotte, V. et al. (Eds). *Climate Change 2021: The Physical*

980 *Science Basis. Contribution of Working Group I to the Sixth Assessment Report of the Intergovernmental Panel on Climate Change*. Cambridge, United Kingdom and New York, USA: Cambridge University Press. pp.817–922. [Online]. Available at: doi:10.1017/9781009157896.008.817.

Tkachuk, R. (1969). Nitrogen-to-protein conversion factors for cereals and oilseed meals. *Cereal Chemistry*, 46, pp.419–424. [Online]. Available at: https://www.cerealsgrains.org/publications/cc/backissues/1969/Documents/chem46_419.pdf.

985 Triboi, E. and Triboi-Blondel, A. M. (2002). Productivity and grain or seed composition: A new approach to an old problem - Invited paper. *European Journal of Agronomy*, 16 (3), pp.163–186. [Online]. Available at: doi:10.1016/S1161-0301(01)00146-0.

Vazquez-Cruz, M. A. et al. (2014). Global sensitivity analysis by means of EFAST and Sobol' methods and calibration of reduced state-variable TOMGRO model using genetic algorithms. *Computers and Electronics in Agriculture*, 100, pp.1–12.

990 [Online]. Available at: doi:10.1016/j.compag.2013.10.006.

Wang, E. and Engel, T. (2002). Simulation of growth, water and nitrogen uptake of a wheat crop using the SPASS model. *Environmental Modelling and Software*, 17 (4), pp.387–402. [Online]. Available at: doi:10.1016/S1364-8152(02)00006-3.

Wang, Y. and Frei, M. (2011). Stressed food - The impact of abiotic environmental stresses on crop quality. *Agriculture, Ecosystems and Environment*, 141 (3–4), pp.271–286. [Online]. Available at: doi:10.1016/j.agee.2011.03.017.

995 Xu, B. et al. (2023). Impacts of meteorological factors and ozone variation on crop yields in China concerning carbon neutrality objectives in 2060. *Environmental Pollution*, 317 (September 2022). [Online]. Available at: doi:10.1016/j.envpol.2022.120715.

Yadav, A. et al. (2019a). The effects of elevated CO2 and elevated O3 exposure on plant growth, yield and quality of grains of two wheat cultivars grown in north India. *Heliyon*, 5 (8), p.e02317. [Online]. Available at:

1000 doi:10.1016/j.heliyon.2019.e02317.

Yadav, D. S. et al. (2019b). ROS production and its detoxification in early and late sown cultivars of wheat under future O3 concentration. *Science of the Total Environment*, 659, pp.200–210. [Online]. Available at: doi:10.1016/j.scitotenv.2018.12.352.

Yadav, D. S. et al. (2020). Responses of an old and a modern Indian wheat cultivar to future O3 level: Physiological, yield and

1005 grain quality parameters. *Environmental Pollution*, 259. [Online]. Available at: doi:10.1016/j.envpol.2020.113939.

Zanis, P. et al. (2022). Climate change penalty and benefit on surface ozone: A global perspective based on CMIP6 earth system models. *Environmental Research Letters*, 17 (2). [Online]. Available at: doi:10.1088/1748-9326/ac4a34.

Zhang, J. et al. (2015). Wheat genotypic variation in dynamic fluxes of WSC components in different stem segments under drought during grain filling. *Frontiers in Plant Science*, 6 (AUG), pp.1–11. [Online]. Available at: doi:10.3389/fpls.2015.00624.

Zhao, D. et al. (2015). Overexpression of a NAC transcription factor delays leaf senescence and increases grain nitrogen concentration in wheat. *Plant Biology*, 17 (4), pp.904–913. [Online]. Available at: doi:10.1111/plb.12296.